Recent Progress in Electrocatalyst for Li-O_2 Batteries

*Zhiwen Chang, Jijing Xu, and Xinbo Zhang**

In the Li-O_2 field, the electrocatalyst plays an important role in accelerating the sluggish electrochemical reactions, thus improving the performances of Li-O_2 battery. In this field, numerous researches regarding the incorporation of electrocatalyst have been published. With the aim to provide an easy as well as timely access for readers to follow the latest development in the catalyst area, the progress regarding the recent development on the application and research of electrocatalyst for Li-O_2 batteries is reviewed in a comprehensive and systematic manner. The application of various kinds of electrocatalyst including solid catalyst and soluble catalyst is first summarized. Then, relevant research including the catalyst design and the correlation between the catalyst property and the Li-O_2 battery performance is discussed. Finally, insights on how to fabricate an effective electrocatalyst are provided, which are expected to provide guidance for further catalyst design.

1. Introduction

Nowadays, on our planet, we are confronted with a daunting challenge caused by the gradual depletion of fossil fuel. To secure a safe and sustainable energy supply, various kinds of renewable and clean energy have been developed, such as solar energy, wind power, hydro electric power, etc. However, the generation of this energy is geographically limited, thus calling for the arrival of efficient energy storage technology, which is further emphasized by the surging demand in extending the driving range of electrical vehicle and individual working lifetime of electronic devices. Under this circumstance, numerous energy storage technologies such as Li-ion battery, Li-S battery, Zn-MnO_2 battery, supercapacitor, etc. have been developed.[1,2] Among them, the Li-ion battery, which is operated based on intercalation mechanism, has played an important role in our society in the past two decades.[3] Despite the progress accomplished to date, however, even when fully developed, the highest energy storage that Li-ion batteries can deliver is too low to meet the demands of key markets, such as transport, in the long term. Reaching beyond the horizon of Li-ion batteries is a formidable challenge. Fortunately, the emergence and development of Li-air battery has provided a solution, benefiting from its much higher theoretical energy density than that of Li-ion battery.[4]

In contrast to the closed system of Li-ion battery, the lithium-air batteries are featured with an open cell structure, in which the cathode active material, oxygen, can be breathed from ambient atmosphere.[5] As a benefit, the weight of the battery is reduced, thus helping to improve the energy density of Li-air battery. To date, the existing Li-O_2 technology can be classified into four groups in terms of the types of electrolyte, including, aqueous, aprotic, aqueous/aprotic hybrid and all solid state electrolyte.[6] And the researches on the aprotic Li-O_2 battery have taken the dominant place, based on which all the discussion mentioned below is all around nonaqueous Li-O_2 battery. For clarity, all the "Li-O_2 battery" mentioned below are "non-aqueous Li-O_2 cell". A typical rechargeable Li-O_2 cell is composed of a Li metal anode, a porous cathode and a non-aqueous Li conducting electrolyte as schematically illustrated in **Figure 1**a. In principle, the electrochemical reaction driving the operation of Li-O_2 battery is $2Li + O_2 \leftrightarrow Li_2O_2$, with the forward direction describing the discharge process and the reverse direction describing the charge.[7] It can be seen that it is the absorption and release of O_2 during the operation of Li-O_2 battery, of which the process cause no damage to the environment. Simultaneously, the electrolytes used, such as tetraethylene glycol dimethyl ether (TEGDME), dimethoxyethane (DME), dimethylsulfoxide (DMSO), is non-toxic and non-corrosive, in sharp contrast with the H_2SO_4 being the electrolyte used in lead-acid battery.[8] All of these have made the nonaqueous Li-O_2 battery a green and environmentally-friendly energy supplier of the next generation. To realize the practical application of Li-O_2 battery, numerous research efforts have been devoted into the Li-O_2 field since the rechargeability of cathode in Li-O_2 battery was demonstrated by Bruce's group.[9] In addition to the deepened understanding on oxygen-based electrochemistry, the performances of Li-O_2 battery have been improved significantly with the help of various strategies over the past decade.[10] Regretfully, the development of this promising Li-O_2 technology is still in its infancy. To realize the final commercialization of Li-O_2 battery, significant efforts in a variety of fields, including reaction mechanisms analysis, electrolyte, cathode, etc., to unlock its full potential are necessary. Among these fields, the incorporation of an effective electrocatalyst is a topic of strategic importance.

According to the established results, the Li-O_2 batteries are still confronted with many challenges, such as low round-trip efficiency, poor rate capability, and limited cycle life etc. (Figure 1b)[11,12] In addition to the influence from electrolyte and anode, these challenges are also caused by the slow kinetics

Z. Chang, Dr. J. Xu, Prof. X. Zhang
State Key Laboratory of Rare Earth Resource Utilization
Changchun Institute of Applied Chemistry
Chinese Academy of Sciences
Changchun 130022, P. R. China
E-mail: xbzhang@ciac.ac.cn

Z. Chang
University of Chinese Academy of Sciences
Beijing 100049, China

DOI: 10.1002/aenm.201700875

of both oxygen reduction reaction (ORR) and oxygen evolution reaction (OER) taking place on the cathode.[13–16] As demonstrated, the incorporation of active cathode catalyst, which can increase the overall energy storage efficiency by accelerating ORR and OER process, makes sense. Currently, many insightful reviews on Li-O_2 battery have been published from various perspectives,[17–22] thus providing an excellent starting point for researchers with the desire to explore the Li-O_2 technology. However, the content reported in these reviews doesn't include the latest development regarding electrocatalyst in Li-O_2 battery. Simultaneously, they also fail to report on the researches of electrocatalyst, including catalysts design and the correlation between the catalyst property and the Li-O_2 battery performance. With the aim to fill in these void, the recent development on the application and research of electrocatalyst for Li-O_2 batteries are reviewed systematically and comprehensively in our progress, being able to provide an easy as well as timely access for readers to follow the latest development in the catalyst area. Bearing these in mind, this article is divided into three sections. In the first section, the latest development associated with solid electrocatalyst and redox mediator is summarized systematically and comprehensivly. Then relevant researches on catalyst design and the catalyst property on the Li-O_2 battery performance are discussed, which should provide insight for powerful catalyst fabrication in the near future. Last but not the least, a body of insights on how to fabricate an effective electrocatalyst are provided.

2. Electrocatalysts for Li-O_2 Battery

As a promising energy storage system, the practical application of Li-O_2 battery has been restricted by many technical challenges, including low round-trip efficiency, degraded capacity and cyclability.[23,24] These challenges are closely related with the sluggish kinetics in generating and oxidizing Li_2O_2 during cycling and the parasitic reactions involving the degradation of the cathode materials and electrolytes.[20,24] In response, considerable research efforts have been devoted to the search for stable electrolytes that can resist the attack of the oxidative species.[25] Meanwhile, intensive endeavors are also devoted into the discovery and application of powerful electrocatalyst, which can accelerate the reaction kinetics associated with Li_2O_2 generation and decompositon, thus enhancing the performances of Li-O_2 battery. In this aspect, various solid catalysts, such as nanostructured carbon materials, metal oxides, heteroatom doped carbonaceous materials etc. and soluble redox mediators have been applied in the Li-O_2 system, followed with success of varying degree.

2.1. Nanostructured Carbon Materials and Heteroatoms Doping Carbon Material

Carbon materials have significant advantages to be used as electrode materials for energy storage devices, including light weight, low cost, and abundant resources.[26,27] In the Li-O_2 field, various carbon materials, such as commercial carbon powders,[28,29] mesocellular carbon aerogels,[30,31] carbon nanofibers and graphene etc.,[32–35] have been applied as cathode. In essence, the cathode made of pure carbon materials can be viewed as electrocatalyst since these carbonaceous materials mentioned above possess good ORR activity. Of note is that, these carbonaceous materials suffer from the lack of advanced architecture. As a result, the mass transfer of all reactants cannot be smoothly promoted and the chemical

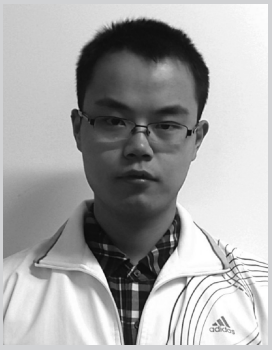

Zhiwen Chang was born in 1987 and received his B.S. degree in materials science and engineering from Dalian Maritime University in 2012. He is currently pursuing a Ph.D. under the supervision of Prof. Xinbo Zhang at Changchun Institute of Applied Chemistry, Chinese Academy of Sciences. His current interests include the synthesis and characterization of nanostructures in lithium–oxygen batteries.

Jijing Xu received his B.S. and Ph.D. degrees in applied chemistry from Jilin University, China, in 2006 and 2011, respectively. He then went to the Changchun Institute of Applied Chemistry (CIAC), Chinese Academy of Sciences (CAS), working as a postdoctor from 2011–2013. As of 2013, he is working as an assistant professor under the direction of Prof. Xinbo Zhang at CIAC, CAS. He is now working as an associate professor at CIAC. His current research interests include the synthesis and characterization of efficient energy storage materials and their application in lithium–air batteries.

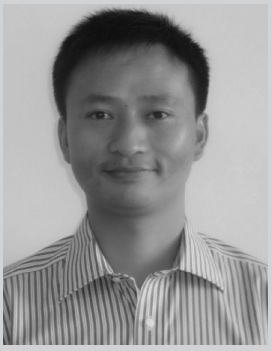

Xinbo Zhang is a Full Professor at Changchun Institute of Applied Chemistry (CIAC), Chinese Academy of Sciences (CAS). He obtained his Ph.D. in inorganic chemistry from CIAC. Before joining CIAC in December 2009, he worked as a Japan Society for the Promotion of Science (JSPS) postdoctoral fellow (2005–2007) and a New Energy and Industrial Technology Development Organization (NEDO) research associate (2007–2009) at National Institute of Advanced Industrial Science and Technology (AIST), Japan. His interests mainly focus on functional inorganic materials for batteries, fuel cells, electrochemical water splitting and carbon dioxide reduction.

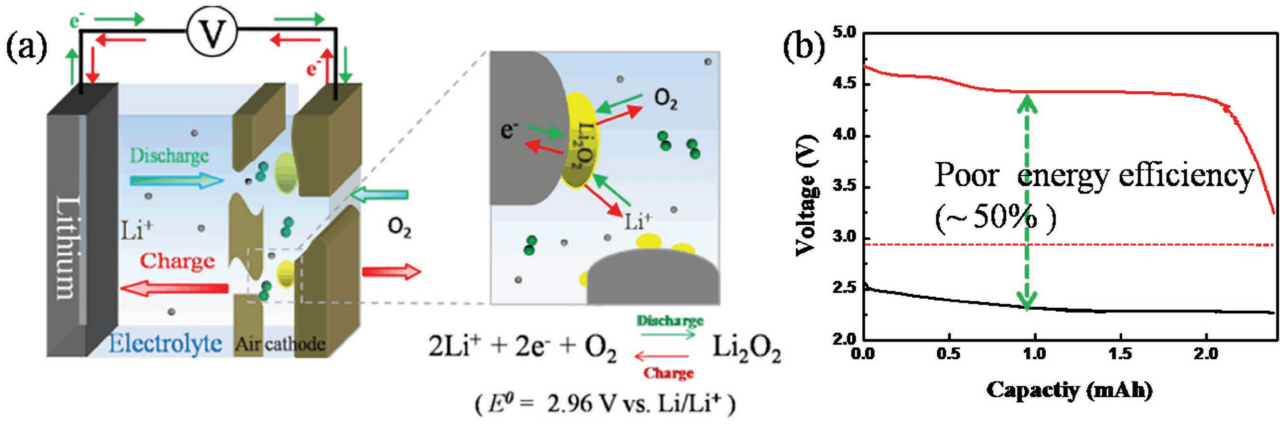

Figure 1. a) A schematic representation of a nonaqueous Li-O_2 battery. b) The first discharge/charge curve of Li-O_2 battery.

pathways can be easily blocked by the deposit of discharge product during discharge. In most cases, Li-O_2 battery with these materials only exhibits undesirable performances such as a low capacity and low-rate capability and so on. To solve this problem, numerous effort has been devoted into developing numerous carbon materials with well-designed structures, such as hierarchical porous graphene,[36,37] mesoporous carbon,[38–40] and hierarchical-fibril carbon nanotubes (CNTs),[41] based on which the Li-O_2 battery has exhibited desirable performances. Among them, several classical nanostructured carbonaceous materials are briefly discussed in the following section. Early in 2011, Xiao et al. reported a hierarchical cathode with functionalized graphene sheets using a microemulsion approach (**Figure 2**a).[42] In contrast to the typically formed two-dimensional layered structure of graphene sheets and composites, the three-dimensional cathode in this work consist of interconnected pore channels on both the micro- and nanometer length scales, which have contributed to the high capacity of the

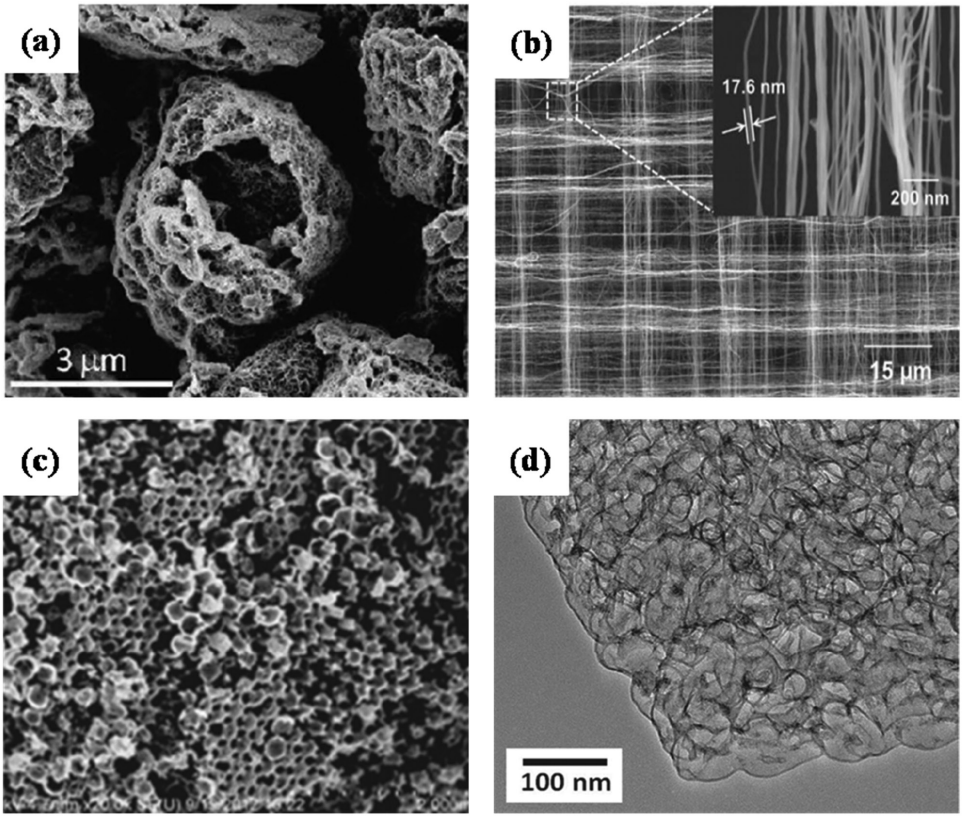

Figure 2. a) SEM images of as-prepared functionalized graphene sheets (FGS) air electrodes. Reproduced with permission.[42] Copyright 2011, American Chemical Society. b) SEM images of the CNT fibril. Reproduced with permission.[44] Copyright 2013, Wiley-VCH. c) SEM image of mesoporous-macroporous carbon sphere arrays (MMCSAs) cathode. Reproduced with permission.[45] Copyright 2013, Wiley-VCH. d) High-magnification TEM images of mesoporous carbon nanocubes. Reproduced with permission.[46] Copyright 2015, Wiley-VCH.

Li-O_2 battery. Since then, several similar researches including the fabrication of a free-standing hierarchically porous carbon (FHPC),[43] a novel carbon air electrode with controlled pore structure (Figure 2b)[44] and a 3D ordered mesoporous-macroporous carbon sphere arrays (MMCSAs) (Figure 2c),[45] have been reported. All of these researches have demonstrated the importance of porous nanostrucures of carbonaceous materials in improving the performance of Li-O_2 battery, which is further verified by Sun.[46] In his research, mesoporous carbon nanocubes are fabricated and applied in Li-O_2 batteries (Figure 2d). By virtue of the numerously hierarchical mesopores and macropores, the oxygen diffusion and electrolyte impregnation throughout the electrode during battery operation are facilitated. When they are applied as cathode catalysts, the Li-O_2 cells can deliver a discharge capacity of 26100 mA h g^{-1} at 200 mA g^{-1}, which is much higher than that of commercial carbon black catalysts. In light of these researches above, the development of porous nanostructures is a promising strategy to improve the electrochemical performance of Li-O_2 batteries. However, the relatively poor ORR/OER activity of pure carbonaceous materials has restricted their further application in the Li-O_2 battery. Luckily, the chemical tuning of the carbon surface property using heteroatoms (e.g., N, S, O or P) has provided a choice.[47–50] It has been computationally and experimentally suggested that the electrocatalytic activity of nanostructured carbon materials towards oxygen electrochemistry is improved after heteroatom doping, due to the interactions between the heteroatom's lone-pair electrons and the carbon π-systems.[51] In this regard, nitrogen doping is particularly attractive thanks to its strong electron affinity and the substantially high positive charge density of the adjacent C atoms. As a benefit, a powerful electrocatalyst with enhanced catalytic activity can be obtained after nitrogen doping, which is verified experimentally.[52–55] In this aspect, several kinds of nitrogen doping materials including N-doped GNSs,[52] nitrogen-doped graphene with sheet-like nanostructure,[53] and nitrogen-doped, onion-like carbon,[54] are reported. All of these researches have exhibited an improvement of varying extent after nitrogen doping.

In light of the researches discussed above, it is desirable to combine the novel structure of carbonaceous materials and tailored composition by nitrogen-doping together, so as to produce a Li-O_2 battery with high performances. Until now, Han has reported the synergistic effect of chemical doping and 3D bicontinuous porous configuration can dramatically improve the electrode reaction kinetics of graphene.[55] While, Zhang et al. prepared a hierarchical carbon–nitrogen architectures with both macrochannels and mesopores, through an economical and environmentally benign sol–gel route, showing high electrocatalytic activity and stable cyclability over 160 cycles in Li-O_2 batteries.[56] In another case, vertically aligned nitrogen-doped coral-like carbon nanofiber (VA-NCCF) arrays were reported by Shui (**Figure 3**a).[57] Thanks to the unique vertically aligned, coral-like N-doped carbon microstructure with a high catalytic activity and an optimized oxygen/electron transportation capability, the Li-O_2 batteries based on this cathode have exhibited an energy efficiency as high as 90% and a narrow voltage gap of 0.3 V between the charge/discharge plateaus. This battery also demonstrates excellent reversibility and cycleability. With years going forward, another work of typical significance is also reported from the same research group in 2016.[58] An efficient cathode with porous nitrogen-doped holey graphene is developed (Figure 3b). Benefiting from the efficient metal-free catalytic activity brought by nitrogen doping and three dimensional mass transport pathway, the resultant Li-O_2 cell can deliver a high round-trip efficiency (85%) and a long cycling life (>100 cycles) under controlled discharge/charge depths or a high capacity of 17 000 mA h g^{-1} under the full discharge/charge condition, superior to most other carbonaceous cathodes. Sharing similarity in catalyst design, Zhao et al. reported the synthesis of 3D porous N-doped graphene aerogels (NPGAs) with frameworks constructed by interconnected nanocages (Figure 3c).[59] Benefiting from the unique structure with broad space and the sufficient N atom active sites within graphene sheets, the as-made NPGA delivers a high specific capacity, an excellent rate capacity of 5978 mA h g^{-1} at 3.2 A g^{-1}, and long cycle stability, especially at a large current density (54 cycles at 1 A g^{-1}). Clearly, recent studies have indicated that Nitrogen doping could be a low-cost, efficient strategy to obtain a good activity for the oxygen reduction reaction (ORR).

In terms of the researches above, the nitrogen doping can enhance the catalytic activity of carbonaceous materials to a certain degree. However, these achieved performances on OER are still far from satisfactory, thus calling for more efforts. In principle, an ideal catalyst for facilitating OER should possess the

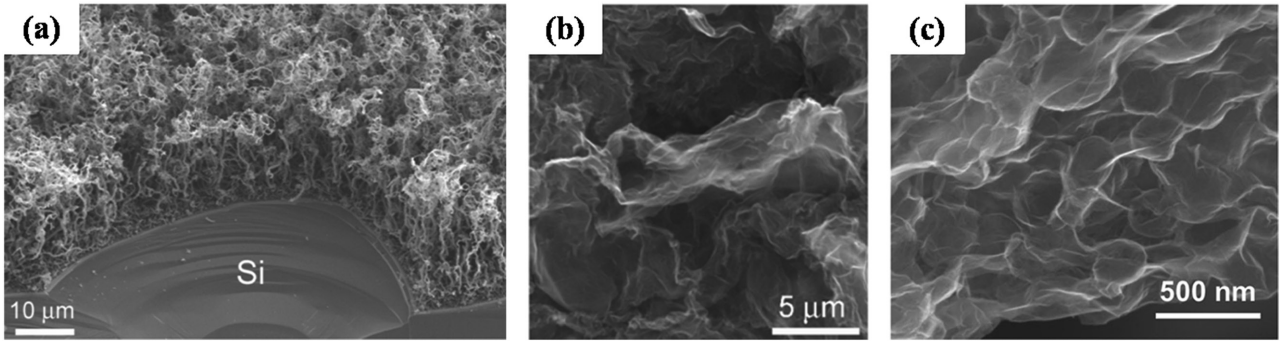

Figure 3. a) SEM image of a vertically aligned nitrogen-doped coral-like carbon nanofiber (VA-NCCF) array grown on a piece of Si wafer by CVD. Reproduced with permission.[57] Copyright 2014, American Chemical Society. b) SEM images of the highly porous N-H Gr electrode from DMF. Reproduced with permission.[58] Copyright 2016, American Chemical Society. c) SEM image of N-doped graphene aerogels (NPGA) cathode. Reproduced with permission.[59] Copyright 2015, Wiley-VCH.

electron-withdrawing ability, which can promote the electrons flow from Li_2O_2 to the substrate. In this aspect, boron-doped graphite carbon may be a good candidate owing to its p-type behavior. Till now, Zhang's group has reported that the boron doped graphene reduced the rate-determining step barrier as a catalytic substrate for Li-O_2 batteries determined by first principles calculation.[60] This may help increase the oxygen evolution rate and improve the rate capability of OER. Simultaneously, the boron-doped graphene is found to have good catalytic activity in decreasing the oxygen evolution barrier demonstrated by Ren et al.[61] However, the role of boron-doped graphite carbon in improving electrochemical performance of Li-O_2 batteries is only theoretically feasible, requiring experimental validation. Correcting this deficiency, Wu reported the 3D porous B-rGO material with a hierarchical structure prepared by a facile freeze drying method.[62] The Li-O_2 battery with the B-rGO achieves good rate capability and cycling life. And the contributions originate from two aspects. On one hand, the successful incorporation of B element into carbon lattices has activated the electrons in the the π system. Benefiting from the p-type behavior, B-rGO promotes charge transfer from Li_2O_2 to the substrate, which decreases energy barriers of rate-determining steps. Meanwhile, B-rGO exhibits a much stronger interaction with the Li_5O_6 cluster, and thus B-rGO activates Li-O bonds to decompose Li_2O_2 more effectively than rGO does during charge, which is verified by the DFT results in **Figure 4**. In theory, the ability of B-rGO catalyst in lowering the overpotential and enhancing the cycling performance can be further improved by adding other catalysts, given the possibility of synergistic effect between different catalysts.

2.2. Noble Metal, Metal Oxides and Other Electrocatalysts

As mentioned above, using pure carbon materials is insufficient to promote the formation/decomposition of Li_2O_2, especially Li_2O_2 oxidation. The sluggish kinetics of oxidizing Li_2O_2 with carbon would induce high overpotential during charge, limiting the reversibility and rate capability of Li-O_2 battery. To counter these challenges, various kinds of catalysts, for example noble metals and their oxides, transition metal oxides, etc. have been incorporated. And their recent progresses will be discussed briefly in the following section.

In the field of Li-O_2 batteries, it is widely accepted that noble metals possess an excellent electrocatalytic activity for ORR and OER. According to the pioneer work by Lu et al., they showed that both charge and discharge overpotentials of Li-O_2 batteries could be obviously reduced by using a bifunctional Pt/Au catalyst, where Pt and Au catalyze OER and ORR, respectively.[63] Since then, the efforts devoted into the application of noble metals and their oxides or alloys has been surging. In this aspect, some relevant literature is summarized in the **Table 1**, which is expected to provide the reader with an easy access to these achievements. In spite of the fact that noble metal or noble metal oxides are proven to be superior ORR and OER catalysts for Li-O_2 battery. However, the problem is the very limited precious metal resources on our earth for large scale commercialization of Li-O_2 battery, not to mention their high prices and the ease of suffering degradations due to poisoning and/or leaching of metals. Alternatively, the development of non-noble metal materials with desirable catalytic activity is a topic of critical importance. In this regard, the reports regarding various transitional-metal oxides, metal carbides, etc. have been surging, of which these latest development is also listed in **Table 2**. Simultaneously, some detailed discussion regarding the application of these catalysts in the Li-O_2 battery is provided in the following section, which is expected to help the readers to access these achievements easily. In light of the published results, some transitional-metal oxides and spinel oxides, including Co_3O_4,[98–101] MnO_2,[102,103] NiO,[104,105] $MnCo_2O_4$,[111,112] $CuCo_2O_4$,[113] $ZnCo_2O_4$[114] etc. are applied in the Li-O_2 battery benefiting from their low cost and catalytic activity. Compared with these materials, the ternary spinel oxide $NiCo_2O_4$ has aroused much interest for use as an electrocatalyst for Li-O_2 batteries thanks to its good electronic conductivity and catalytic activity.[115,116] So far, various kinds of $NiCo_2O_4$-based electrocatalyst are reported,[117–122] including hierarchical $NiCo_2O_4$ nanorods,[117] hierarchical macroporous/mesoporous $NiCo_2O_4$ nanosheets,[118] have been reported. As a typical example among these researches, Gong et al. has reported a high-loading $NiCo_2O_4$ nanoparticles (NCONP) anchored on three-dimensional N-doped graphene as an efficient bifunctional catalyst for Li-O_2 battery.[120] In his research, the introduction of the rGO can create the high surface area, which give a good performance for ORR and improve the electrical conductivity between the NCONPs. The as-synthesized

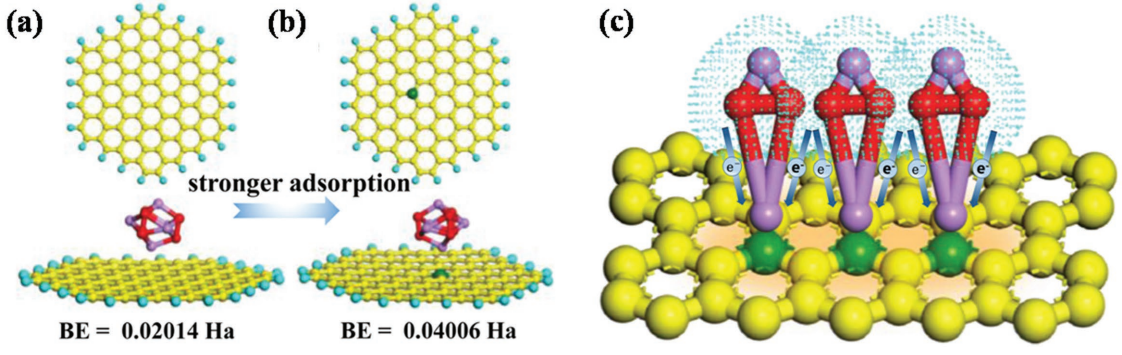

Figure 4. Optimized geometries of the Li_5O_6 cluster and a) rGO, b) B-rGO. Corresponding binding energy values are also listed. c) Schematic picture of B-rGO as the substrate gaining electrons from the Li_2O_2. Reproduced with permission.[62] Copyright 2016, American Chemical Society.

Table 1. Summary of the noble metal/metal oxides used in nonaqueous Li-O_2 batteries.

Material	Substrate	Performance	Year	Ref.
Pt	Hierarchical CNT cathode	100 cycles with full discharge and charge	2013	[64]
	α-MnO_2	A good cycling stability and low charge potential	2014	[65]
	Hollow graphene nanocages	The charge voltage plateau can reduce to 3.2 V at 100 mA g^{-1} and maintain below 3.5 V when the current density increased to 500 mA g^{-1}	2016	[66]
	N-doped single wall CNT	A high discharge capacity of 7685 and 5907 mA h g^{-1} at 100 and 500 mA g^{-1}, respectively, and also good capacity retention	2016	[67]
Pd	Hollow spherical carbon deposited onto carbon paper	213 cycles at a rate of 300 mA g^{-1} and a capacity of 1000 mA h g^{-1}	2013	[5]
	TiO_2 nanowire arrays grown onto carbon textiles	Desirable performances	2015	[7]
	Super P	The charge overpotential is reduced to ~0.2 V	2013	[68]
	CNTs	100 cycles at a fixed capacity of 1000 mAg/g_{carbon}	2015	[69]
	Graphene nanoplatelets	30 cycles	2016	[70]
	Nitrogen-doped carbon-nanofiber	High capacity, low overpotential and good cycling stability	2016	[71]
	Hollow graphene nanocages		2016	[72]
	NiO nanomembranes	409 cycles at a current density of 500 mA g^{-1}, an overpotential of 0.47V between the charge and discharge voltage	2016	[73]
	MnO_x–GeO_y nanomembranes	160 cycles and an extremely low charge voltage of only ~3.14V	2016	[74]
Ru	Carbon black	150 cycles with the capacity limited to 100 mA h g^{-1}	2016	[75]
	Porous graphene	200 cycles with the capacity limited to 100 mA h g^{-1} and a high reversible capacity of 17700 mA h g^{-1}	2014	[76]
	Caronized bacterial cellulose	20 cycles with a capacity cut-off value of 500 mA h g_{total}^{-1} at 200 mA g^{-1}	2015	[77]
	Mesporous graphene-like carbon	A capacity about 6433 mA h g^{-1} at a current density of 200 mA g^{-1}	2016	[78]
	Graphene nanosheets@Ni foam	Over 200 cycles with a low overpotential of 0.23 V under the capacity curtained to be 1000 mA h g^{-1} at a current density of 200 mA g^{-1}	2016	[79]
	Hierarchically ordered macro-mesoporous carbon	A high specific capacity of 12 400 mA h g^{-1} at a current density of 200 mA g^{-1} and an excellent cycling performance up to 100 cycles at 400 mA g^{-1} with the restricted capacity at 1000 mA h g^{-1}	2016	[80]
Ir	Deoxygenated hierarchical graphene	150 cycles with a limited capacity of 1000 mA h g^{-1} at a current density of 2000 mA g^{-1}	2015	[81]
	Graphene oxide	A low charge overpotential about 3.2V, 40 cycles	2016	[82]
Au	CNT	Desriable perfromances.	2016	[83]
	Cracked carbon tube arrays	Good rate capability (1208 mA h g^{-1} at a high current density of 1000 mA g^{-1}) and long cycle life (112 cycles at a current density of 400 mA g^{-1} with a limited capacity of 500 mA h g^{-1})	2016	[84]
	Graphene	300 times at 400 mA g^{-1} with the capacity limited at 500 mA h g^{-1}	2016	[85]
RuO_2	Reduced Graphene oxide	30 Cycles at the high current density of 500 mA g^{-1} and high specific capacity of 5000 mA h g^{-1}	2013	[86]
	CNT	73% electrical efficiency	2013	[87]
	KB+dendrimer	Good performance	2014	[88]
	Nitrogen-doped graphene	100 discharge/charge cycles at the cutoff capacity of 2000 mA h g^{-1} and low average charge potential of 3.7 V	2015	[89]
	Ordered mesoporous carbon nanofiber arrays	High capacity (20600 mA h g^{-1} at a current density of 100 mA g^{-1}) high rate (9750 mA h g^{-1} at a current density of 1000 mA g^{-1}) and long-life (300 cycles at a fixed capacity of 1000 mA h g^{-1})	2015	[90]
	Vertically aligned carbon nanotube	A superior rate capability and cycling stability	2016	[91]
	Mn_2O_3 nanorods	Good performance	2016	[92]
Alloy	Pt_2Ru	Good performance	2014	[93]
	AgPd-Pd	A good cycling performance and reduce charge voltage	2015	[94]
	Pt_3M (M = 3d, 4d and 5d transitionmetals)	Low ORR and OER overpotentials	2016	[95]
	PdM(M = Fe, Co, Ni)		2017	[96]

Table 2. Summary of the non-noble materials catalyst used in nonaqueous Li-O_2 batteries.

Materials	Performance	Year	Ref.
Co_3O_4	Reduced charge voltage and increased specific capacity	2013	[98]
	A high discharge capacity of 4500 mA h g^{-1} at a current density of 123 mA g^{-1}. Over 200 cycles at a current density of 246 mA g^{-1} with a limited capacity of 740 mA h g^{-1}.	2015	[99]
	Higher specific capacity and better cycling stability over 54 cycles at 100 mA g^{-1}.	2016	[100]
	This composite structure exhibited enhanced performance with a specific capacity of 2453 mA h g^{-1} at 0.1 mA cm^{-2} and 62 stable cycles with 583 mA h g^{-1} (1000 mA h g^{-1}_{carbon}).	2016	[101]
MnO_2	Over 90 cycles with a capacity of more than 1000 mA h $(g_{MnO2})^{-1}$ and a high coulombic efficiency of around 100% in the voltage rang of 2.2 and 4.4 V.	2014	[102]
	A high discharge capacity of 3660 mA h g^{-1} at 0.083 mA cm^{-2} and 132 cycles at a capacity of 492 mA h g^{-1} (1000 mA h g^{-1}_{carbon}) with low overpotentials under a high current density of 0.333 mA cm^{-2}. A high average energy density of 1350 W h Kg^{-1} is maintained over 110 cycles at this high current density.	2014	[103]
NiO	70 cycles	2015	[104]
	A stable cycling with 40 cycles with no obvious performance decay	2015	[105]
Mo_2C/CNT	The efficiency is up to 88% with a cycle life of more than 100 cycles	2015	[106]
MoS_2	85% round-trip efficiency and 50 cycles	2016	[107]
LaSrMnO layers throughout a graphene foam	High specific capacity, superior rate capability, and cyclic stability	2016	[108]
MoO_2/Mo_2C nanocrystal decorated N-doped carbon foam	A high round-trip efficiency of 89.1% (2.77 V/3.11 V) at 100 mA g^{-1} as well as exceptional rate performances and good cyclability in Li-O_2 battery.	2016	[109]
$FePO_4$	Good rate performance, high specific capacity, and perfect cycling stability	2016	[110]
$MnCo_2O_4$	A good cycling stability over 200 cycles	2017	[111]
	Good cycling stability	2013	[112]
$CuCo_2O_4$	Over 80 cycles with the capacity restricted at 500 mA h g^{-1} and much lower charge overpotential and a high capacity up to 5288 mA h g^{-1}	2016	[113]
$ZnCo_2O_4$	A good cycling cyclability and high specific capacity	2015	[114]
$NiCo_2O_4$	Low charge over-potential, high discharge capacity and high-rate capability	2013	[117]
	High reversible capacity, lower charge/discharge overpotential and a good cycling stability	2014	[118]
	An initial capacity of 29280 mA h g^{-1} and retained a capacity of >1000 mA h g^{-1} after 100 cycles.	2016	[119]
$NiCo_2O_4$ anchored onto the N-reduced graphene oxide	A high specific capacity (6716 mA h g^{-1}), great rate performance, and excellent cycling stability with cutoff capacity of 1000 mA h g^{-1} (112 cycles)	2016	[120]
$NiCo_2O_4$@$La_{0.8}Sr_{0.2}MnO_3$ coreeshell structured nanorods	80 cycles at a high current density of 200 mA g^{-1}	2016	[121]
3-D foam-like $NiCo_2O_4$	a relatively high round-trip efficiency of 70% and high discharge capacity of 10 137 mA h g^{-1} at a current density of 200 mA g^{-1}	2017	[122]
graphene-metal hydroxide hybrid arrays	High specific capacity, long cyclability and low charge potentials.	2016	[123]
TiC-C composites	A good specific capacity of 3460 mA h g^{-1} and a good cyclability of 90 cycles	2016	[124]
FeCo-CNT	high efficiency and capacity	2016	[125]

NCO@N-rGO composites deliver a specific surface area (about 242.5 m^2 g^{-1}), exhibiting three-dimensional (3D) porous structure, which provides a large passageway for the diffusion of the oxygen and benefits the infiltration of electrolyte and the storage of the discharge products. Benefiting from these special architectures features and intrinsic materials, the NCO@N-rGO cathode delivers a high specific capacity (6716 mA h g^{-1}), great rate performance, and excellent cycling stability with cutoff capacity of 1000 mA h g^{-1} (112 cycles) in the lithium–oxygen batteries. In addition, $NiCo_2O_4$@$La_{0.8}Sr_{0.2}MnO_3$ coreshell structured nanorods and self-assembled 3D foam-like $NiCo_2O_4$,[121,122] are reported by Yang et al. and Wu et al., respectively, both of which have exhibited desirable performances in terms of the rate capability and cycling stability. To a certain degree, all of these researches have evidenced the promising application of $NiCo_2O_4$ as efficient electrocatalyst in Li-O_2 battery. Simultaneously, these researches also highlights the importance of favorable cathode structure and intrinsically high catalytic activity of cathode material, which is further supported by Zhu et al.[123] In detail, they reported a new electrode structure constituted of vertically aligned carbon nanosheets and metal hydroxide ($M(OH)_x$@CNS) hybrid arrays, integrating

Table 3. A brief summary of the perovskite catalyst used in nonaqueous Li-O_2 batteries.

Materials	Performance	Year	Ref.
$LaFeO_3$	A low overpotential, high specific capacity, good rate capability and cycle stability up to 124 cycles.	2014	[132]
$La_{0.75}Sr_{0.25}MnO_3$	a high specific capacity, superior rate capability, and good cycle stability.	2013	[133]
$La_{0.5}Sr_{0.5}CoO_{3-x}$	A good rate capability and excellent cycle stability of sustaining 50 cycles at a current density of 0.1 mA cm^{-2} with an upperlimit capacity of 500 mA h g^{-1}	2015	[134]
$LaNi_{0.9}M_{0.1}O_3$ (M = Cu, Co)	A high round-trip efficiency and good cycling stability	2017	[139]
Ni-doped $La_{0.8}Sr_{0.2}Mn_{1-x}Ni_xO_3$	A good specific capacity and cycle life	2016	[140]
$La_{1.7}Ca_{0.3}Ni_{0.75}Cu_{0.25}O_4$	Efficient Li_2O_2 oxidation	2012	[144]
$Sr_2CrMoO_{6-\delta}$	High specific capacity, low overpotential and good cyclability	2014	[145]

both favorable ORR and OER active materials. The resulting porous $M(OH)_x$@CNS hybrid nanostructures possess high conductivity, high surface area translating to high electrolyte/electrode interfaces, connected interstitial cavities allowing efficient ion/O_2 transportation, and strongly bound CNS and $M(OH)_x$ nanoparticles. With the $M(OH)_x$@CNS cathode architecture, the Li-O_2 battery has exhibited excellent properties with long cyclability, low charge overpotentials and high specific capacity of 5403 mA h g^{-1} and 12123 mA h g^{-1} referenced to the carbon and $M(OH)_x$ weight, respectively. To a certain degree, this strategy of creating ORR and OER bifunctional catalysts in a single conductive hybrid component have paved the way to efficient cathode catalysts for Li-O_2 battery, which may find their application in other metal-air batteries, as well.

Among all the candidates, perovskite based compound oxides (ABO_3), have attracted increasing attention because of their favorable structural/chemical flexibility, excellent catalytic activity with improved oxygen mobility, and much reduced cost, making them promising alternatives to noble metals as the bifunctional catalysts in Li-O_2 batteries. Till now, various kinds of perovskites including $Sr_{0.95}Ce_{0.05}CoO_{3-x}$, $La_{0.8}Sr_{0.2}MnO_3$, Sr_2CrMoO_{6-x} etc., have been applied in Li-O_2 batteries.[126–131] However, in many cases, perovskite catalysts obtained by conventional synthesis methods have quite low intrinsic electronic conductivities and small specific surface areas, which lead to low catalytic activity, thus limiting their usage. Therefore, to improve the performance of the perovskite materials in Li-O_2 batteries, a variety of modification methods were employed, including (a) combination of ABO_3 with conductive nanocarbons such as carbon black, carbon nanotube, and graphene to enlarge the effective contact area for catalysis and improve the electrical conductivity of the perovskite oxide/carbon electrodes; (b) synthesis of porous-structured perovskites with increased number of oxygen pathways and specific surface area to enhance the catalytic performance. In this aspect, several characteristic porous pervoskites listed in **Table 3** including 3 dimensional order mesoporous $LaFeO_3$ (3DOM LFeO) and $La_{0.75}Sr_{0.25}MnO_3$ nanotubes, a hierarchical mesporous/macroporous perovskite $La_{0.5}Sr_{0.5}CoO_3$ (HPN-LSC) nanotube via electrospinning technique followed by postannealing (**Figure 5**).[132–134] Benefiting from the high catalytic activity and hierarchical mesoporous/macroporous nanotubular structure, the Li-O_2 batteries with these pervoskite have exhibited desirable performances of varying degree. These results will benefit for the future development of high-performance Li-O_2 batteries using hierarchical mesoporous/macroporous nanostructured perovskite-type catalysts. (c) doping in A or B site of ABO_3 to introduce various changes including oxygen vacancies as well as the mixed valence state of B-site metal ion to improve the electrocatalytic activity.[135] Among the aforementioned methods, the doping method deals with the intrinsic properties of the material and has been proved facile and effective. With this method, oxygen vacancies can be easily introduced into the material, which helps to modify the B–O bond and the surface configuration, promoting the ORR and OER.[136,137] Moreover, the introduced oxygen vacancies, as reaction active sites, can facilitate the migrations of both e^- or Li^+ and firmly bind O_2 and Li_2O_2 during the repeated discharge–charge process, bringing improved catalytic performance.[138] In this regard, Pham et al. reported the transition-metal-doped perovskite oxide $LaNi_{0.9}M_{0.1}O_3$ (M = Cu, Co) nanosheets.[139] Thanks to a combination of abundant lattice strain and the oxygen vacancy effect caused by substitution of an element with a different valence state in Ni sites, $LaNi_{0.9}Cu_{0.1}O_3$ catalyst grown on nickel foam exhibits a significant ORR and OER, showing improvement in non-aqueous systems compared with pure $LaNiO_3$ and $LaNi_{0.9}Co_{0.1}O_3$. Similarly, a nickel-doped $La_{0.8}Sr_{0.2}Mn_{1-x}Ni_xO_3$ nanoparticle containing abundant oxygen vacancies is also demonstrated to be an optimized bifunctional catalyst in Li-O_2 batteries.[140]

Recently, studies on the perovskite oxides have offered a new direction in accelerating the ORR and OER kinetics. Compared with the general perovskite oxides, the double perovskite catalyst with a general formula of $AA'B_2O_{5+\delta}$ demonstrates much higher oxygen ion diffusion rate and surface exchange coefficient.[141–143] Lee and co-workers tested the electrochemical activity of a layered perovskite oxide, $La_{1.7}Ca_{0.3}Ni_{0.75}Cu_{0.25}O_4$ (LCNC), in the oxidation of solid Li_2O_2.[144] They demonstrated that compared with the perovskite oxide $La_{0.8}Sr_{0.2}MnO_3$, the LCNC-containing electrode showed a lower charge potential. In addition, the battery with the LCNC-containing electrode delivered higher capacities and exhibited improved capacity retention during cycling compared to that with the catalyst-free electrode. Yuan and coworkers reported the application of the double perovskite oxide $Sr_2CrMoO_{6-}\delta$ which exhibited a higher discharge capacity, lower overpotentials, better rate capability and cycle performance, and higher reversibility than those of Super P.[145]

2.3. Soluble Electrocatalyst

The reduction of the overvoltage upon charging is the key step in the further development of Li-O_2 batteries, providing

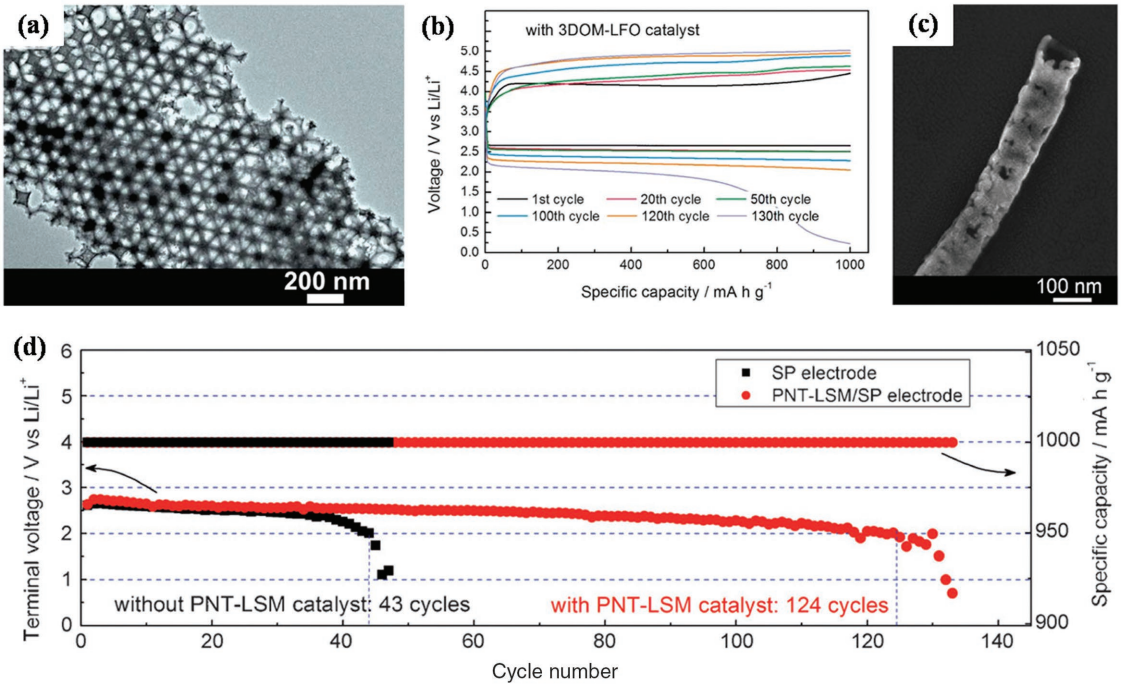

Figure 5. a) TEM image of a 3 dimensional order mesoporous $LaFeO_3$ (3DOM-LFO). b) Cycling response of the Li-O_2 cells with 3DOM-LFO/SP electrodes under a specific capacity limit of 1000 mA h g^{-1}_{carbon}. Current density: 0.15 mA cm^{-2}. Reproduced with permission.[132] Copyright 2014, The Royal Society of Chemistry. c) SEM images of the highly porous $La_{0.75}Sr_{0.25}MnO_3$. d) Voltage of the terminal discharge vs the cycle number for Li-O_2 cells with and without perovskite-based porous $La_{0.75}Sr_{0.25}MnO_3$ nanotubes (PNT-LSM) catalyst at 0.15 mA cm^{-2}. Reproduced with permission.[133] Copyright 2013, Wiley-VCH.

not only a higher efficiency but also a better cycling stability. Until now this strategy was mainly pursued by the use of solid catalysts of various types as summarized above. However, one thing of note is that, the limited contact area between the solid catalyst and the deposited Li_2O_2 has restricted the electron flow during OER, thus leading to generally low catalytic activities. In this aspect, the application of a redox mediator (RM), which can provide oxidative attack at the much larger and dynamic interphase between Li_2O_2 and the liquid electrolyte, has provided a proper solution to this challenge mentioned above. So far, a series of dissolved redox mediators have been used in Li-O_2 batteries, which can be divided into two categories including electron-hole transfer agents and electrocatalyst in terms of the role of redox mediators in the Li-O_2 battery. For the first time, the tetrathiafulvalene (TTF), which acts as an electron–hole transfer agent that permits efficient oxidation of solid Li_2O_2, is introduced into the Li-O_2 system by Bruce et al.[146] In his research, during the charge process, the TTF molecule is oxidized to TTF^+ at the positive electrode and then, in turn, oxidizes the insulating solid Li_2O_2 (which formed in the porous cathode during the previous discharge); at the same time, TTF^+ is reduced back to TTF. By using a molecular electron–hole transfer agent, a far more effective oxidation of Li_2O_2 is possible than can be achieved in its absence. As a result, the cell with the electron–hole transfer agent demonstrated a huge reduction in the charge overpotential than the cell without the TTF does (**Figure 6**a). Since then, the interest in the usage of redox mediator, which mainly acts as electrocatalyst, has been surging followed by numerous researches. For example, a soluble catalyst lithium iodide (LiI) in tetraglyme with porous carbon nanotube fibrils is reported by Lim et al.[147] According to the author, the expected redox mediator reaction is one in which iodide I^-) ions are initially oxidized on the electrode surface to I_3^- or I_2 while charging. Subsequently, the oxidized reactors (I_3^+ or I_2) chemically react with Li_2O_2, producing Li^+ and O_2 gas, with a reverse reaction into the initial iodide (I^-) ions and realized a Li-O_2 battery delivering a high reversible capacity (1000 mA h g^{-1}) up to 900 cycles with reduced polarization (about 0.25 V). Later on, another kind of mobile catalyst, the 2,2,6,6-tetramethylpiperidinyloxyl (TEMPO), is applied in rechargeable Li-O_2 batteries and exhibited a distinct reduction of the charging potentials by 500 mV compared with the Li-O_2 batteries without TEMPO (Figure 6b).[148] While Sun has evidenced the feasibility of organic-electrolyte-dissolved iron phthalocyanine (FePc) as a solution-phase bifunctional catalyst for both discharge and charge processes in lithium–oxygen batteries. It acts not only as a redox mediator, but also as a molecular shuttle of $(O_2)^-$ species between the surface of the electronic conductor and the insulator Li_2O_2 product of discharge.[149] The Li_2O_2 is observed to grow and decompose without direct contact with carbon, which greatly enhances the electrochemical performance. In addition, other kinds of soluble catalyst for Li_2O_2 oxidation, such as LiBr, tris{4-[2-(2-methoxyethoxy)ethoxy]phenyl}amine (TMPPA), tris[4-(diethylaminophenyl]amine (TDPA) etc., are also applied in the Li-O_2 battery, followed by improved performances.[150–152]

Unlike other soluble catalyst that can accelerate the OER reactions, the 2,5-di-*tert*-butyl-1,4-benzoquinone (DBBQ) is a kind of ORR electrocatalyst.[153] It can promote the solution

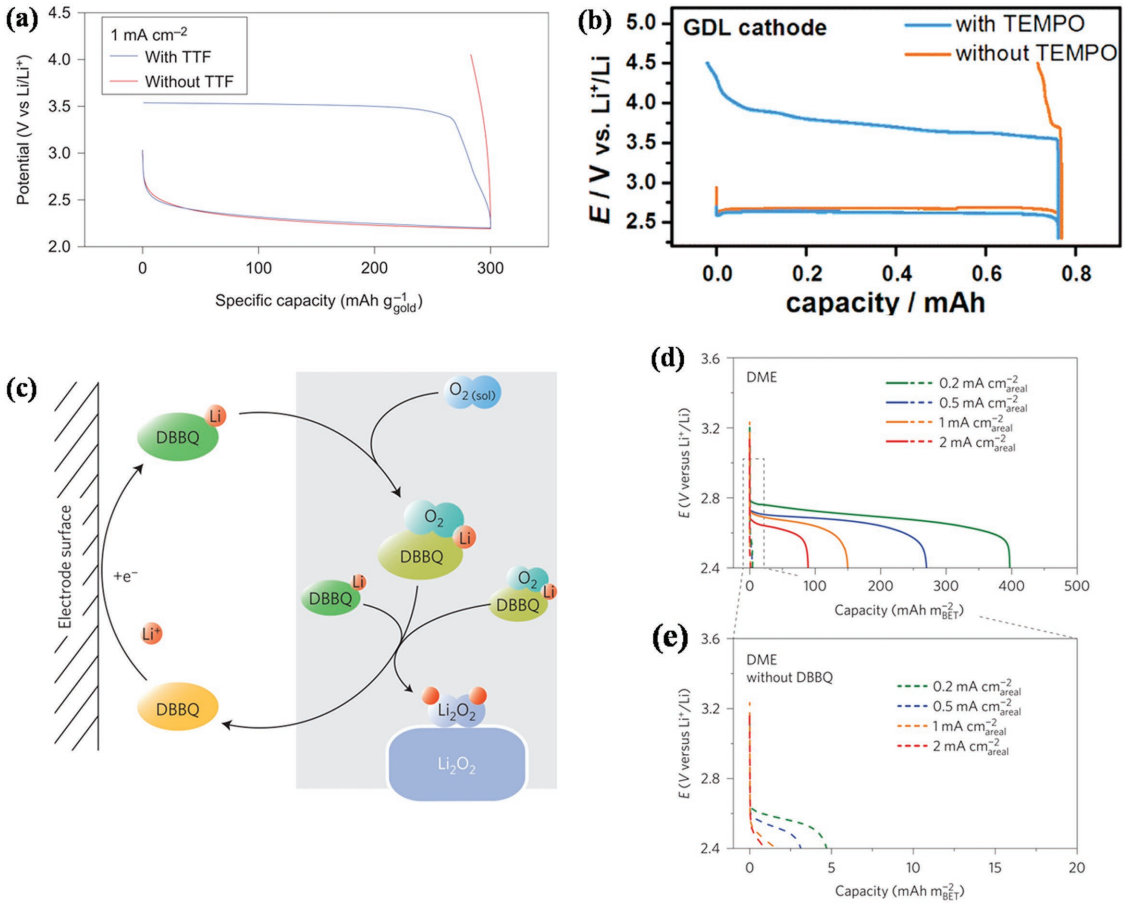

Figure 6. a) First-cycle load curves (constant-current discharge/charge) with and without TTF at 1 mA cm^{-2} Reproduced with permission.[146] Copyright 2013, Macmillan Publishers Limited. b) A gas diffusion layer (GDL) cathode and a charge current density of 0.1 mA cm^{-2}. Reproduced with permission.[148] Copyright 2014, American Chemical Society. c) Schematics of the reaction on discharge with 2,5-di-*tert*-butyl-1,4-benzoquinone (DBBQ). d) Load curves of oxygen reduction at a gas diffusion electrode discharged in 1 M LiTFSI in DME with 10 mM DBBQ (solid lines) and without DBBQ (dashed lines) under O_2 at various areal current densities from 0.1 mA cm^{-2} to 2 mA cm^{-2}. e) Enlarged section of the load curves recorded without DBBQ in b. Reproduced with permission.[153] Copyright 2016, Macmillan Publishers Limited.

growth of Li_2O_2, thus suppressing direct reduction to Li_2O_2 on the cathode surface, which would otherwise lead to Li_2O_2 film growth and premature cell death. As illustrated in Figure 6c, upon discharge, the DBBQ is reduced at the electrode surface, forming LiDBBQ, and then LiDBBQ reacts with O_2, producing Li_2O_2 and itself being regenerated to DBBQ. As a benefit, the incorporation of DBBQ halves the overpotential during discharge and increase the capacity 80- to 100-fold and enables rates >1 mA cm^{-2}_{areal} for cathodes with capacities of >4 mA h cm^{-2}_{areal} (Figure 6d,e). More significantly, the application of DBBQ additive can enhance the stability of carbonaceous cathode and electrolyte in the Li-O_2 battery indirectly, since it operates by a new mechanism that avoids the oxidative LiO_2 intermediate in solution.

3. Design Principle and Catalyst Descriptor

In the above section, we have discussed the application of various kinds of catalysts in the Li-O_2 battery. In this section, we divide this section into two main parts in terms of the researches of catalyst in the battery. We first review the catalyst design, mainly including the catalyst immobilization and activity enhancement through introducing defects or oxygen vacancies. The correlation between the catalyst properties and the Li-O_2 battery performance is followed, with highlighting the importance of finding a proper catalyst descriptor in guiding the synthesis or selection of powerful catalyst.

3.1. Electrocatalyst Design

The generated discharge product Li_2O_2 can precipitate on the cathode, which can bury the catalytic sites on the cathode gradually. As a result, electron transport through the insulating Li_2O_2 products become difficult, leading to a large ohmic loss and a corresponding increase in the overpotential during charging. Therefore, to effectively preserve catalysts and avoid deactivation after discharge, tailored design and effective positioning of catalyst materials on the oxygen cathode should

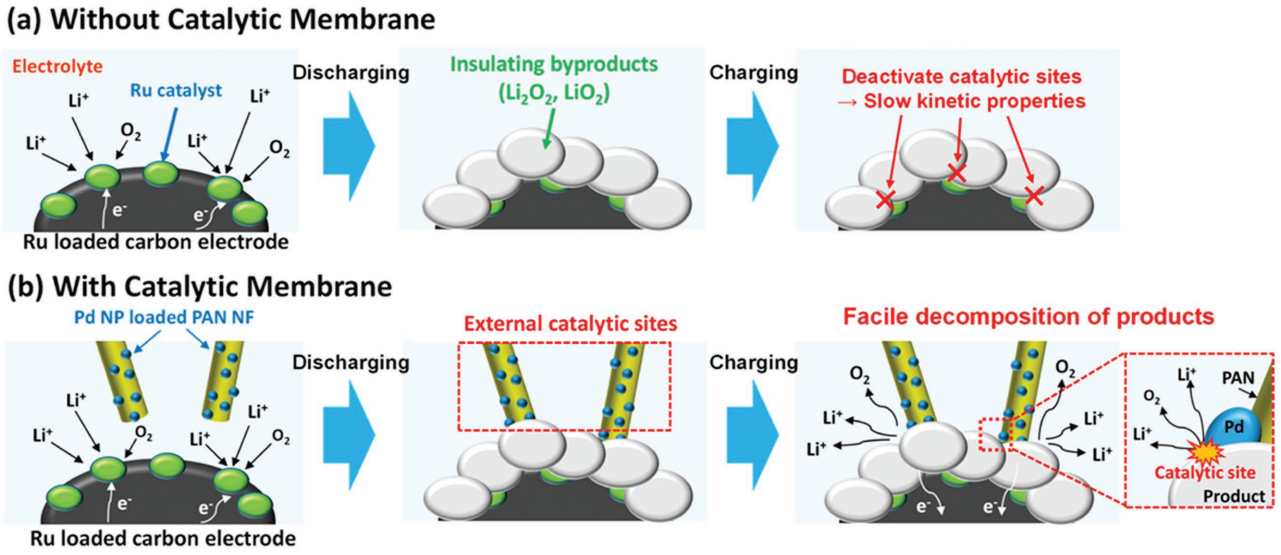

Figure 7. Proposed Reaction Schematic of an Oxygen Electrode a) without and b) with a Catalytic Membrane during Discharging and Charging. Reproduced with permission.[154] Copyright 2015, American Chemical Society.

be required. In this aspect, Ryu et al. has introduced a new Li-O_2 cell architecture that employs a catalytic polymer-based membrane between the oxygen electrode and the separator.[154] As illustrated in **Figure 7**, the discrete Pd/PAN membrane continuously affords catalytic sites once Pd NPs near the electrode are embedded in the generated Li_2O_2. Simultaneously,

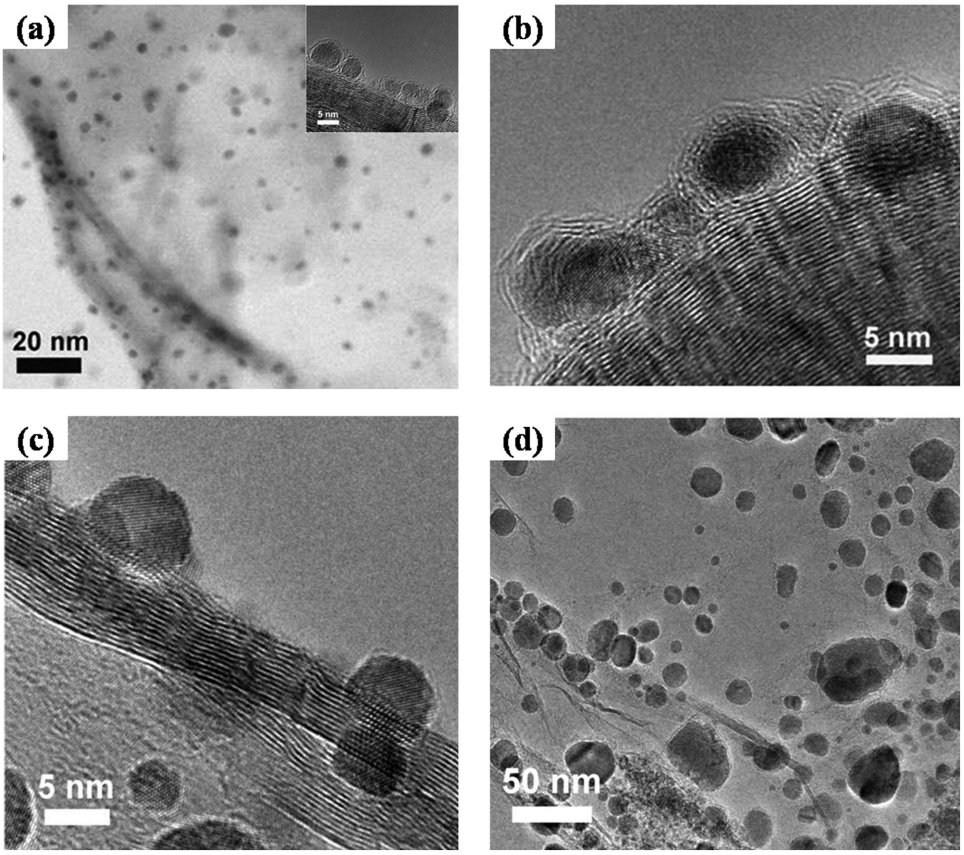

Figure 8. a) TEM image of nanoporous N-doped graphene nanosheets with uniformly dispersed encapsulated RuO_2 nanoparticles with the inset being High-resolution TEM of the RuO_2 nanoparticles surrounded by 2–3 layers of N-doped graphene. b) High-resolution TEM of the RuO_2 surrounded by 2–3 layers of N-doped graphene at the charge state after 50 cycles. c) High-resolution TEM image of the un-encapsulated RuO_2 nanoparticles before test. d) TEM images of the unencapsulated RuO_2 nanoparticles after 62th cycles. Reproduced with permission.[155] Copyright 2015, Wiley-VCH.

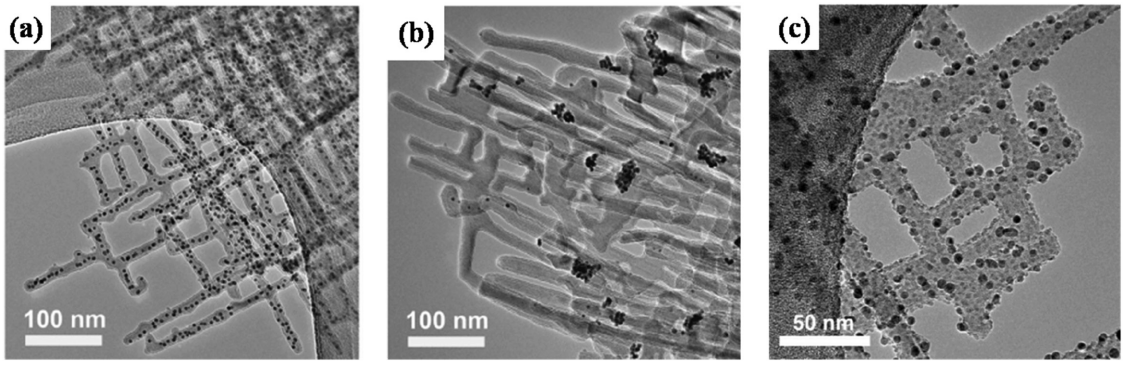

Figure 9. Transmission electron micrographs of Pd/$TiSi_2$ nanonets a) as-grown and b) after 63 cycles of discharge/recharge. c) TEM image of Pd/Co_3O_4/$TiSi_2$ cathode after 60 cycles still exhibited good dispersion of Pd nanoparticles. Reproduced with permission.[160] Copyright 2015, American Chemical Society.

during charge, the exposed Pd NPs can serve as the active sites to decompose Li_2O_2. As a benefit, the Li-O_2 cell with a catalytic membrane showed an extended cyclability and a reduced polarization (≈0.3 V) compared to cells without a catalytic membrane. In general, the solid catalyst is usually decorated on carbonaceous oxygen cathode to provide catalytic sites which are necessary for ORR/OER. However, in some cases, the weak bonding between nanoparticulate catalysts and the carbonaceous materials by physical adsorption can lead to the coarsening and agglomeration of catalytic nanoparticles during the cycling of Li-O_2 battery. As a result, the performances of Li-O_2 are worse due to the catalyst deactivation. To address this challenge, Guo has encapsulated the RuO_2 nanoparticles with nanoporous nitrogen-doped graphene.[155] Compared to the pristine electrode, the RuO_2 nanoparticles do not show obvious coarsening and are still encapsulated by 2–3 layers of N-doped graphene, demonstrating the high stability of the hybrid nanostructure (**Figure 8**a,b). In sharp contrast, unencapsulated RuO_2 nanoparticles suffer from serious aggregation and coarsening after about 62 cycles (Figure 8c,d), failing to support the cell reactions. To a considerable extent, the improved stability of RuO_2 nanoparticles has contributed to the long life (100 cycles) of Li-O_2 battery with the encapsulated RuO_2 nanoparticles, nearly doubling the life of Li-O_2 battery with the unencapsulated RuO_2 nanoparticles (62 cycles). Clearly, the encapsulation in carbon matrix effectively prevents the coarsening of the catalyst nanoparticles after cycles, promoting the cyclic stability of Li-O_2 battery. In this aspect, several researches including Co-Ni catalysts encapsulated with carbon nanofiber,[156] the Mo_2C nanoparticles wrapped with carbon coating,[157] the encapsulation of RuO_2 nanoparticles by CNTs,[158] the CoO nanoparticles confined into bimodal mesoporous carbon,[159] have been reported. As a typical example among them, Yao et al. has added a layer of Co_3O_4 to stabilize the Pd nanoparticles on the $TiSi_2$ nanonets.[160] In light of their report, due to the poor adhesion of Pd nanoparticles to the $TiSi_2$ nanonets, serious Pd detachments and aggregation take place during the cycling of Li-O_2 battery. In sheer contrast, with the protection of functional Co_3O_4 layer, the Pd nanoparticles are effectively immobilized and no obvious changes to the morphology or distribution of Pd nanoparticles can be observed even after 60 cycles of discharge/recharge, thus helping to preserve the activity of Pd nanoparticles. It can be seen that the Pd/Co_3O_4/$TiSi_2$ combination affords the desired functionalities and stability compared to the Pd /$TiSi_2$ ones. Finally, the Li-O_2 battery with Pd/Co_3O_4/$TiSi_2$ has exhibited a doubled cycling lifetime than the Li-O_2 battery with Pd /$TiSi_2$, extending from 63 cycles to 126 cycles (**Figure 9**).

It is quite necessary to enhance the Li-O_2 batteries performances by accelerating the ORR and OER process with the help of catalyst. To this end, the activity of the catalyst should be enhanced, which can be achieved by introducing defects or oxygen vacancies. Nazar et al. developed a novel metallic mesoporous oxide with a fraction of surface defects, which demonstrates a lower charge potential for OER.[161] So far, various kinds of catalysts containing vacancies and/or defects,[162–165] such as oxygen vacancy-bearing MnO_2,[163] vacancy-rich $MnCo_2O_4$,[164] and oxygen vacancy-bearing CoO (CoO-A),[165] have been reported. To be specific, in the research by Gao et al., a successful synthesis of oxygen vacancy-bearing CoO (CoO-A) through a simple calcination of $Co(Ac)_2 \cdot 4H_2O$ in

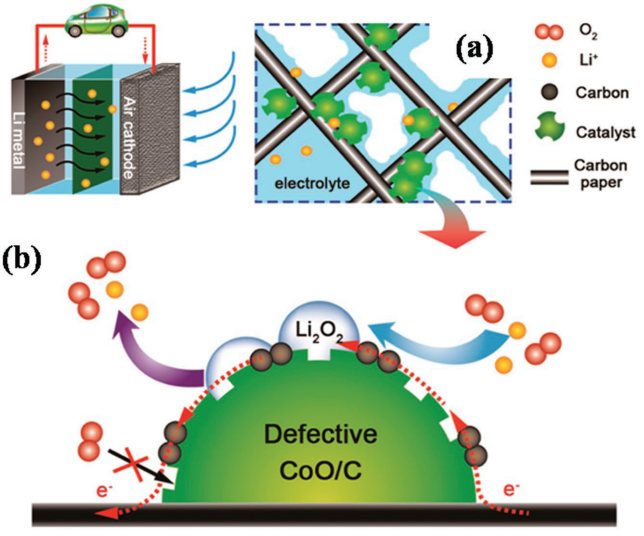

Figure 10. a) Schematic of the CoO/C-based air cathode. b) Synergetic mechanism of the dotted carbon and oxygen vacancies in CoO/C on ORR and OER. Reproduced with permission.[166] Copyright 2016, American Chemical Society.

Ar.[165] In comparison with defect-free CoO-N derived from the decomposition of $Co(NO_3)_2 \cdot 6H_2O$, an oxygen-deficient CoO-A based cathode shows much higher cycling stability, higher rate capability, higher coulombic efficiency, and lower charge-discharge overpotential. However, in that work, the initial capacity at a current density of 200 mA g^{-1} was only 3421 mA h g^{-1} due to the limited ORR activity. Furthermore, the overpotential also markedly increased after 20 cycles. To correct this deficiency, in the same research group, a novel strategy to enhance the catalytic activity of CoO through the integration of carbon species and oxygen vacancies is proposed.[166] In comparison with the commercial or oxygen-vacancies-only CoO, the electrochemical performances of CoO/C-catalyzed cathode, such as cycling stability, the initial capacity, have all been greatly enhanced, thanks to the synergistic effect of the dotted carbon species and oxygen vacancies on ORR and OER. In detail, the oxygen vacancies can enhance the mobility of e^- and Li^+ and bind to O_2 and Li_2O_2 as active sites. The dotted carbon species not only improve the conductivity of CoO but also stabilize the oxygen vacancies during ORR/OER, of which the mechanism is schematically illustrated in **Figure 10**. In consistence with the results, Luo et al. also demonstrated the improved performance of Li-O_2 battery with the aid of oxygen vacancies.[167] In his study, the oxygen vacancies are created by a facile heat treatment of rutile TiO_2 (H-TiO_2). Thanks to the presence of defects, the adsorption and dissociation of oxygen are facilitated. As a

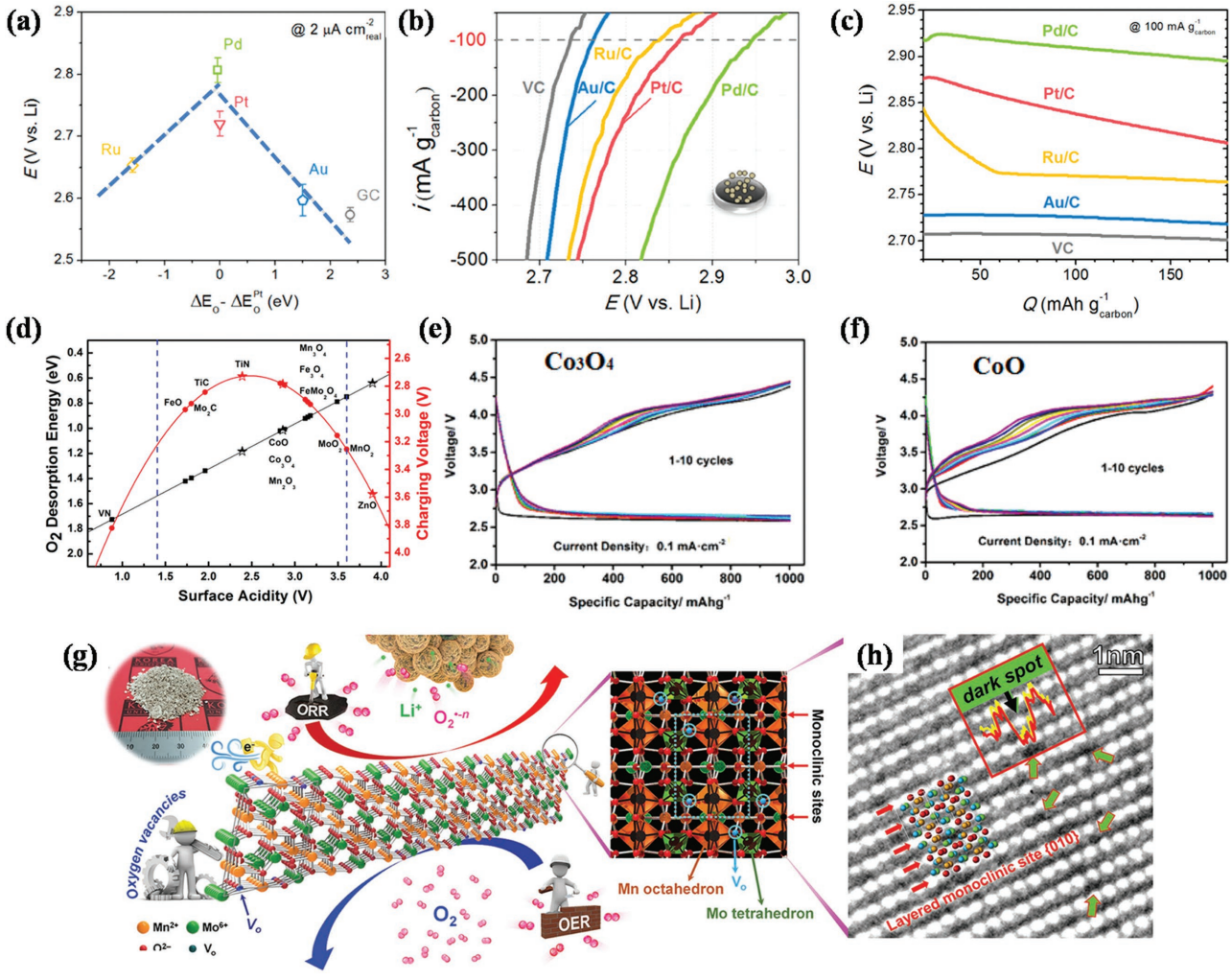

Figure 11. a) Nonaqueous Li^+-ORR potentials at 2 μA cm^{-2} real as a function of calculated oxygen adsorption energy, ΔEO, relative to that of Pt. b) Background- and IR-corrected ORR polarization curves of Pd/C, Pt/C, Ru/C, Au/C, and VC thin films on GC (0.05 mg_{carbon} cm^{-2}_{disk}) in O_2-saturated 0.1 M $LiClO_4$ in DME at 900 rpm and 5 mV s^{-1}. c) Initial discharge profiles of Li-O_2 cells of Pd/C, Pt/C, Ru/C, Au/C, and VC at 100 mA g^{-1}_{carbon}. Reproduced with permission.[168] Copyright 2011, American Chemical Society. d) Predicted catalytic activities of some transition-metal compounds (TMC: oxides, carbides, and nitrides) based on the established correlation of O_2 desorption and charging voltage with surface acidity. All values were calculated based on surface acidity, although charging voltages and O_2 desorption energies of TiN, Co_3O_4, and ZnO have been calculated before e) Discharging and charging profiles of the Co_3O_4. f) Discharging and charging profiles of the CoO. Reproduced with permission.[176] Copyright 2015, American Chemical Society. g) Digital photograph of gram-scale $MnMoO_4$ nanowires after co-precipitation for 60 min (P60-MMO) and schematic illustration of the ORR/OER. h) HRTEM image of P60-MMO along the [201] zone axis; its corresponding atomic model is illustrated in the inset (red dots represent the O elements in layered monoclinic sites {010} and the other colored dots represent the O elements in spare sites; oxygen vacancies are indicated using green arrows). Reproduced with permission.[178] Copyright 2016, Wiley-VCH.

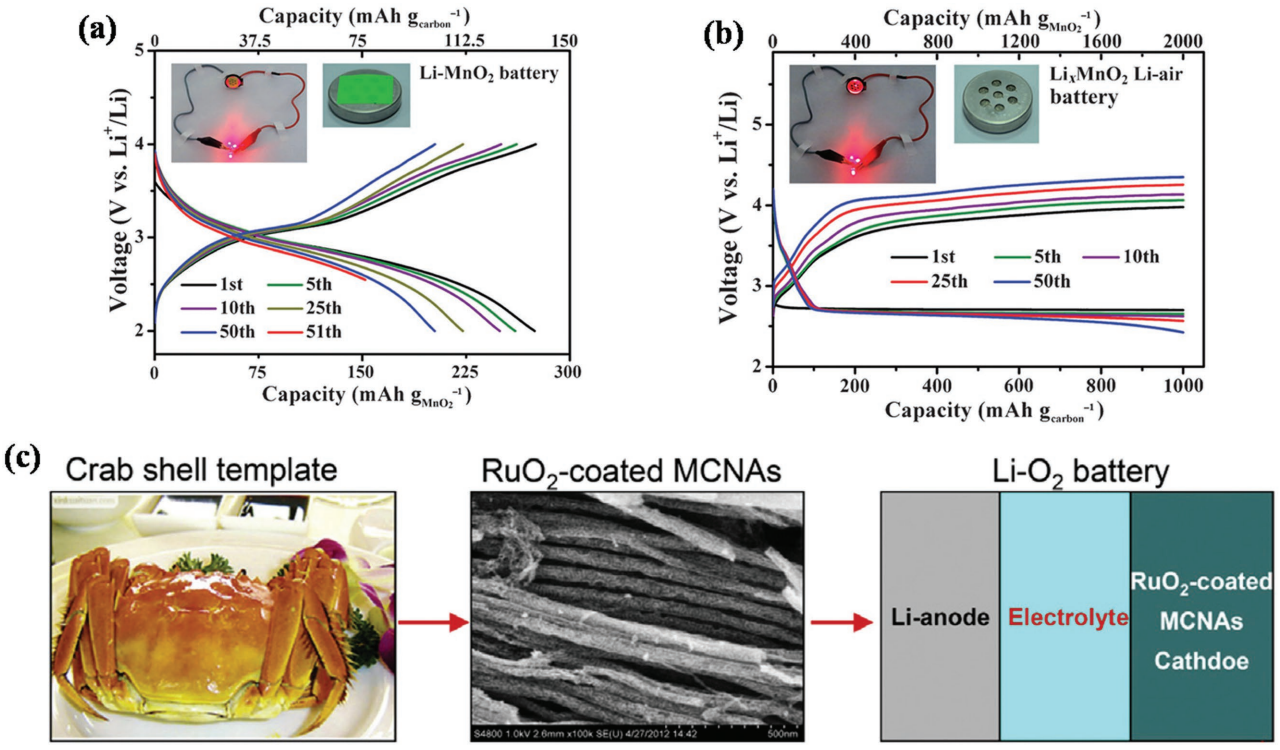

Figure 12. Discharge and charge curves of mesoporous MnO_2-based electrodes in a) a Li-MnO_2 battery and b) a Li-air cell. The Li-MnO_2 cell was cycled between 2.0 and 4.0 V for 50 cycles and ceased to a discharged state of $Li_{0.50}MnO_2$. The same cell was then exposed to air and was discharged/charged at a current density of 100 mA g_{carbon}^{-1}. Insets show photographs of the assembled batteries powering light emitting diodes. Reproduced with permission.[180] Copyright 2015, Wiley-VCH. c) Graphic illustration of the electrode synthesized with the crab shell template. Reproduced with permission.[181] Copyright 2015, Elsevier.

benefit, the Li-O_2 battery with H-TiO_2 can be discharged at the current densities of 0.3 and 0.5 mA cm^{-2} while maintaining the specific capacities of 3.2 and 2.8 mA h cm^{-2}, respectively, much higher than those of the batteries with pristine rutile TiO_2.

3.2. Correlation Between Electrocatalyst Property and Li-O_2 Battery Performance

In recent years, to obtain a Li-O_2 battery with high power and high round-trip efficiency, many research efforts have focused on the use of solid and liquid catalysts to reduce the overpotentials in aprotic Li-O_2 batteries. After years of research, some properties of the catalyst are reported to affect the performance of Li-O_2 battery significantly. Early in 2011, Shao-Horn et al. performed systematic studies on the intrinsic ORR activity of polycrystalline palladium, platinum, ruthenium, gold, and glassy carbon surfaces in 0.1 M $LiClO_4$ 1,2-dimethoxyethane via rotating disk electrode measurements.[168] They found that the nonaqueous Li^+-ORR activity of these surfaces primarily correlates to oxygen adsorption energy, forming a "volcano-type" trend. Moreover, the activity trend found on the polycrystalline surfaces was in good agreement with the trend in the discharge voltage of Li-O_2 cells catalyzed by nanoparticle catalysts (**Figure 11**a–c). Later, Xu et al. performed extensive first-principle calculation for these catalytic mechanisms of noble metals and revealed consistent trend of catalytic activity.[169,170] The high active catalyst should have an appropriate O adsorption strength close to those of well-established Pt and Pd catalysts. Other kinds of factors which can correlate with the performances, such as the catalyst size,[171,172] the crystal facet,[173,174] and the conductivity are reported.[175] Among these efforts, Zhu

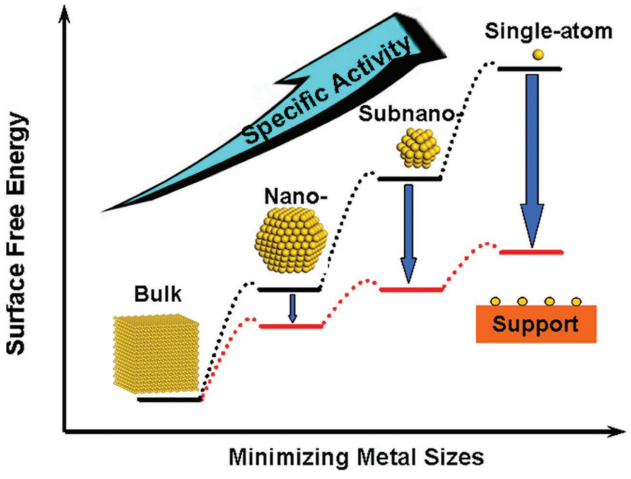

Figure 13. Schematic illustrate the changes of surface free energy and specific activity per metal atom with metal particle size and the support effects on stabilizing single atoms. Reproduced with permission.[183] Copyright 2013, American Chemical Society.

et al. reported that the certain materials with an appropriate surface acidity can achieve the high catalytic activity in reducing charging voltage and activation barrier of rate-determinant step.[176] In his research, the surface acidity of transition-metal compounds (TMC: oxides, carbides, and nitrides) is strongly correlated with the corresponding charging voltage and desorption energies of Li^+ and O_2 over TMC (Figure 11d–f). According to this correlation, CoO is predicted to be as active as Co_3O_4 in reducing charging overpotential, confirmed by their comparative experimental studies. Encouragingly, in light of this correlation, other TMCs (Co_3O_4, TiC, TiN) are predicted to have a relatively high catalytic activity, being consistent with the previous experiments. However, in our opinion, the low charge overpotential can be caused by the different Li_2O_2 morphology, or the defect in Li_2O_2. Despite being so, the present study enables the rational design of catalysts with greater activity for charging reactions of Li-O_2 battery. In the same year, Zheng et al. reported the oxygen sites on the surface play a more important role than the exposed metal sites, since lithium ions from electrolytes interact with the surface oxygen sites and form surface lithium sites, facilitating further growth of Li_2O_2.[177] The catalytic activity of $MnMoO_4$ is strongly correlated with its surface oxidation state for multiple metal cations containing oxygen vacancies with respect to the electrochemical performance.[178] $MnMoO_4$-containing intrinsic oxygen vacancies is shown to offer a very high catalytic activity for reversible ORR/OER in

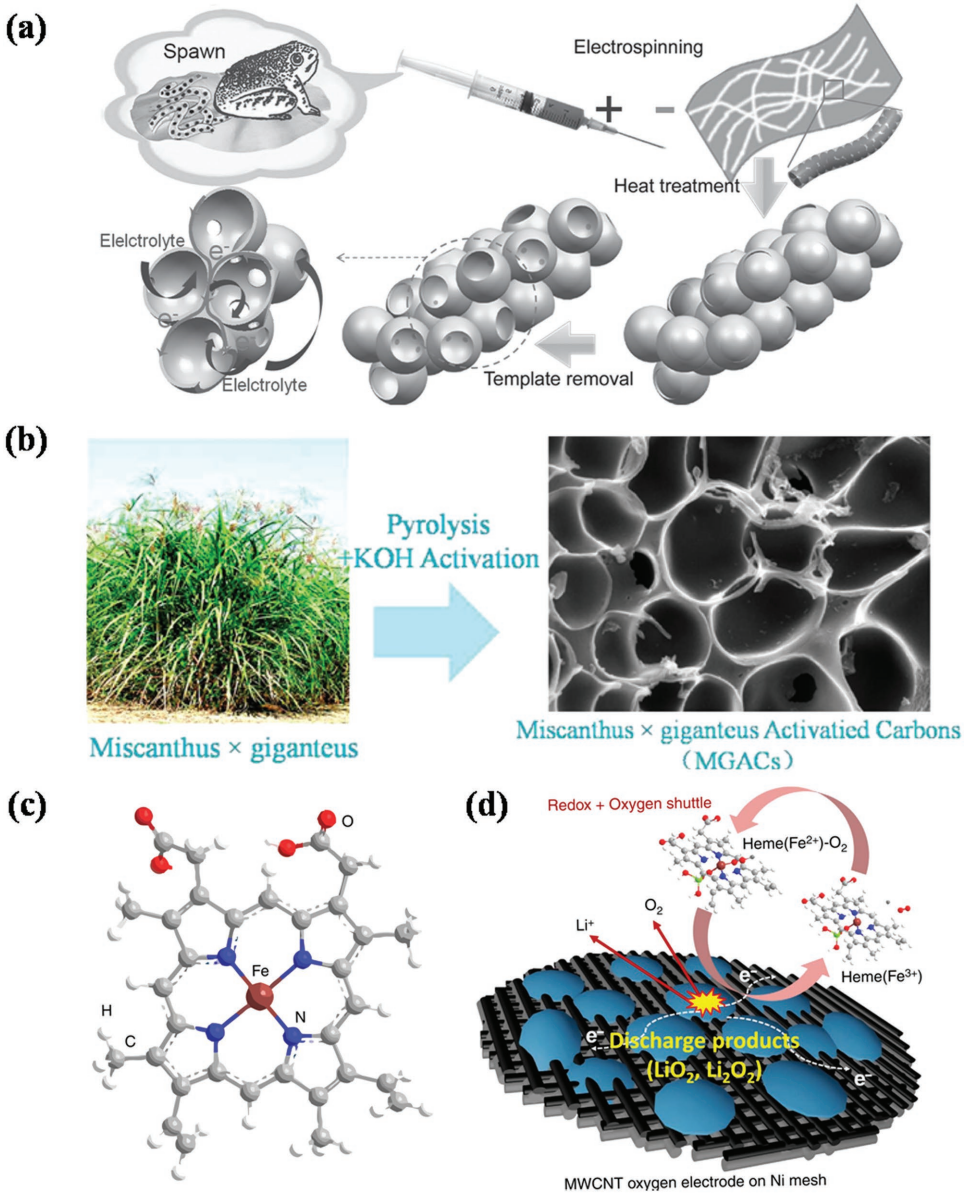

Figure 14. a) A schematic illustration of the fabrication process and motivation of the macroporous hollow active carbon fiber cathode. Reproduced with permission.[184] Copyright 2016, Wiley-VCH. b) Graphic illustration of the synthesized materials. Reproduced with permission.[185] Copyright 2017, American Chemical Society. c) Structure of heme molecule. d) Schematic illustration of oxygen electrode charged in the heme-containing Li-O_2 cell. Reproduced with permission.[186] Copyright 2016, Macmillan Publishers Limited.

the Li-O_2 cell, of which the possible mechanism is illustrated in Figure 11g,h. They have successfully shown the fast ORR/OER kinetics, long-term cycle stability (over 180 cycles at 1000 mA g_{sp}^{-1}), and superior rate capability (3000 mA g_{sp}^{-1} for 70 cycles) at a fixed capacity of 1000 mA h g_{sp}^{-1} of $MnMoO_4$. Clearly, with the help of a proper strategic design principle, an effective catalyst can be found or fabricated with ease. And such a rule not only applies to the solid catalyst mentioned above, but also is applicable to the selection of RM. According to Lim et al.[179] a general design principles for finding a soluble catalyst is proposed and their validity is demonstrated using DFT calculations and experimental verification. The ionization energy (I.E.) was suggested as the key descriptor for designing a catalyst, where specific organics with a certain range of I.E. values (5.8–6.8 eV) can be used as soluble catalysts. Furthermore, the HOMO energy level of the catalyst should be considered in comparison with the formation energy of Li_2O_2 and the HOMO energy level of the electrolyte. Based on this guideline, 5,10-dimethylphenazine (DMPZ) was successfully identified with a remarkably low overpotential and high stability in the Li-O_2 cell. We believe that the verification of key factors for designing a RM will open up a new avenue for the development of effective novel catalysts and advanced Li-O_2 batteries with high efficiency and long cycle life.

Even though, these researches are carried out individually from different aspects, along with their achievements, their established results can still provide guidance for our further researches. Of note is that the design and facile synthesis of efficient cathode catalysts to accelerate the sluggish kinetics of both oxygen reduction reaction (ORR) and oxygen evolution reaction (OER) are still a big challenge for lithium–air batteries that needs to be overcome.

4. Summary and Outlook

In the energy storage field, the Li-O_2 battery holds the potential to be the energy supplier of the next generalization, benefiting from its ultrahigh energy density. During the past decade, intensive efforts have been devoted into the research and development of Li-O_2 battery with the dream to realize its practical application. Regretfully, the commercialization of Li-O_2 battery is still hindered by a variety of technical hurdles, such as low obtainable capacity, poor energy efficiency, and limited cycle life. To address these problems, along with enhancing cathode and electrolyte stability, the sluggish kinetics of ORR and OER need to be accelerated as well. In response, effective catalyst should be incorporated. So far, various kinds of catalysts including carbonaceous materials, noble metal/metal oxides, RM etc. have been reported, of which their progress are summarized briefly and systematically in this progress. Despite the achievements already made, the development of electrocatalyst for Li-O_2 battery is confronted with some challenges, which are similar to those in the water splitting device, given the involved oxygen species and their interactions with the catalysts in these two systems. To be specific, these challenges that need to be overcome include the fabrication of electrocatalyst with large specific area, high electrical conductivity, good catalytic activity, and deepened understanding on the catalytic mechanism etc. To realize the advantages regarding the energy density of Li-O_2 battery as much as possible, several issues should deserve our attention and action.

First, the origin in obtaining catalysts should be diversified. To realize a green and sustainable Li-O_2 electrochemistry, it is desirable to obtain the catalyst from daily waste. In this regard, some related researches including the application of electrode materials in depleted Li-MnO_2 batteries (**Figure 12**a,b),[180] carbonized bacterial cellulose,[77] the hierarchical porous carbon nanofiber arrays obtained by using natural crab shell template in Figure 12c,[181] the recoverable TiO_2 nanowire arrays cathodes,[182] have been reported. Inspired by these researches, other kinds of materials such as α-Fe_2O_3 from the rust, ZnO from the failed Zn-air battery, should be also good source for the catalyst materials. Simultaneously, the single atom catalyst and two-dimensional material may find their application in the Li-O_2 battery as well. In general case, the single-atom catalyst (SAC) refers to the catalysts that isolated metal atoms singly dispersed on the support (metal oxides, metal surfaces, and graphene etc.), as schematically illustrated in **Figure 13**. Compared with the clusters catalyst, the SACs maximize the efficiency of metal atom use and reduce the cost, which is particularly important for supported noble metal catalysts. And more information regarding SACs can be obtained from reference,[183] which is not described in detail our manuscript. In light of the information above, chances are great that interesting phenomenon and/or surprising results can be obtained when the SACs are applied in Li-O_2 batteries since the SACs offer great potential for achieving high activity and selectivity. We are curious that will the generation of LiO_2 be promoted and that of Li_2O_2 be suppressed during the discharge? During charge, can the discharge products Li_2O_2 and/or Li_xO_y be effectively decomposed? Can the side products especially the Li_2CO_3 and/or LiOH from electrolyte decomposition be effectively depleted with the help of SACs? And these questions also exist when the two-dimensional materials are applied in Li-O_2 batteries.

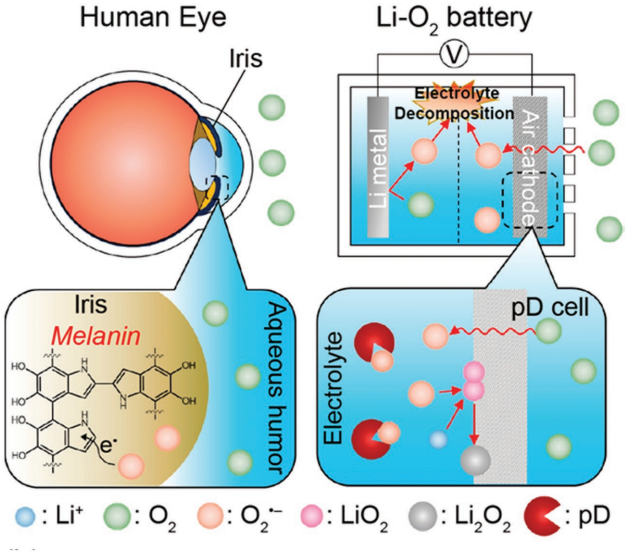

Figure 15. Schematic illustrations comparing Li–O_2 battery with the human eye. The analogous situations of both systems suggest an approach of using pD, a synthetic melanin, as a superoxide radical scavenger. Reproduced with permission.[187] Copyright 2014, American Chemical Society.

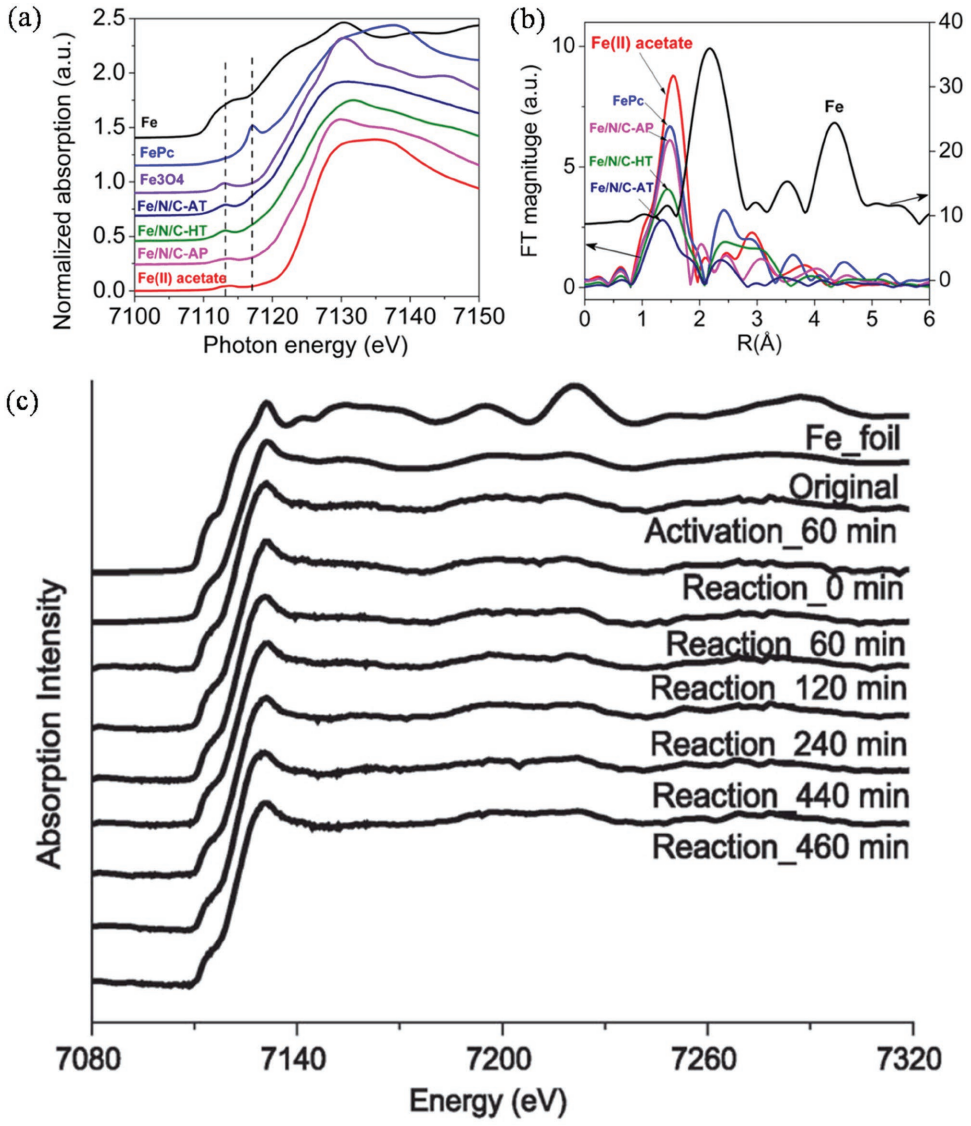

Figure 16. a) Normalized XANES (X-ray absorption near-edge structure) of Fe/N/C-AP (as-prepared precursor), -HT(after heat treatment), and –AT (after the second heat treatment) with reference compounds at the Fe K-edge. b) Magnitudes of k3-weighted Fourier-transformed (phase-uncorrected) EXAFS (extended X-ray absorption fine structure), data for Fe/N/CAP, -HT, and -AT with some reference compounds. Reproduced with permission.[192] Copyright 2012, American Chemical Society. c) In situ Fe K-edge XANES of Pod-Fe cathode under polymer electrolyte membrane fuel cells (PEMFC) operation conditions. Reproduced with permission.[193] Copyright 2013, Wiley-VCH.

Second, we may get inspiration from nature in the pursuit of active catalyst material. So far, several researches such as the fabrication of macroporous interconnected hollow carbon nanofibers inspired by golden-toad eggs[184] (**Figure 14**a), the preparation of activated carbons based on the natural plant miscanthus giganteus (MG)[185] (Figure 14b) and the soluble redox catalyst of heme molecule (Figure 14c,d)[186] have been reported. To be specific, the authors have shown that heme molecule, a common porphyrin cofactor in blood, can function as a soluble redox catalyst and oxygen shuttle for efficient oxygen evolution in non-aqueous Li-O_2 batteries.[168] The heme's oxygen binding capability facilitates battery recharge by accepting and releasing dissociated oxygen species while benefiting charge transfer with the cathode. Similarly, in Li-O_2 field, Kim et al. has proposed a solution to the problems caused by superoxide radical by learning from the human eye (**Figure 15**).[187] In detail, the generated superoxide radical during the cycling of Li-O_2 batteries can cause serious chemical degradation of nearly all cell components of electrolytes, binders, and carbonaceous electrodes, by parasitic reactions. As a result, the performances, which include the cycling stability, round-trip efficiency etc., of Li-O_2 batteries can be impaired. Inspiringly, thanks to the similarity in the situations of both human eye and Li-O_2 system, the defense mechanism against radical attack in human eye is successfully applied in this Li-O_2 batteries. In this research, polydopamine (pD), which is one of the most common synthetic melanins, is introduced in the ether-based electrolyte. As an outcome of the superoxide radical scavenging by the pD

additive, the irreversible side reaction products were alleviated significantly, resulting in superior cycling performance. Taken together, these researches have provided a message that simple treatments inspired by our nature or human body could be an effective, eco-friendly and sustainable solution to the problems in the Li-O_2 systems. In addition, other catalyst mechanisms such as the oxygen spillover effect reported in oxidizing CO at low-temperature and other field,[188,189] and enzyme catalyst mechanisms may be also applicable in the Li-O_2 system, given the involvement of oxygen species during reactions in these systems.

Third, the fundamental understanding of the oxygen reaction mechanisms during operation of Li-O_2 batteries should be deepened. Nowadays, many researchers have applied advanced in-situ techniques to probe the Li-O_2 reactions to elucidate a detailed mechanism. For example, with the help of in situ SERS technique, Bruce et al. has evidenced directly that the surface mechanism in low-DN solvents.[190] Recently, using aberration-corrected environmental transmission electron microscopy (TEM), Luo et al. has imaged the product morphology evolution on a carbon nanotube (CNT) cathode of a working solid-state Li–O_2 nanobattery and correlated these features with the electrochemical reaction at the electrode.[191] In addition, the revealed electronic as well as atomic structure of Fe/N/C composite with X-ray absorption spectroscopy (**Figure 16**a,b) and an intact metallic iron in Pod-Fe after running for 7 h in polymer electrolyte membrane fuel cells (PEMFC) demonstrated with in situ X-ray absorption near-edge structure (XANES) (Figure 16c) have provided critical information for the ORR and OER mechanisms,[192,193] which can support the further study. However, it should be noted that a clear description of their interaction with the reactive intermediates is still not established, which is believed to retard the development of Li-O_2 battery to a certain degree, thus calling for more efforts so as to provide guidance for effective electrocatalyst design.

Honestly speaking, all the challenges with the current Li-O_2 batteries cannot be resolved with the only help of effective catalysts, since the properties of other battery components such as Li anode, cathode etc. can affect the performances as well. Clearly, to obtain a Li-O_2 battery with desirable performance, the influence of these components should be taken into account simultaneously without considering them individually. For these considerations, the mechanisms of Li anode and cathode are discussed briefly. The desired reactions at the anode are the stripping (during discharge) and plating (during recharge) of lithium. However, in the harsh environment of Li-O_2 battery, the high reactivity and low redox potential of Li dictate that complex side reactions often take place when Li is in contact with other chemicals. According to the previous report, the Li can react with the electrolyte and the O_2 as well as H_2O dissolved in the electrolyte, thus leading to serious Li corrosion and consumption.[194–196] With regard to the mechanisms on the cathode, it can be roughly divided into two groups involving the influence of morphology and activity. First of all, a high electronic conductivity of electrode is a factor of critical importance, which can reduce the overall resistance of the air electrode, resulting in a small IR polarization and helping to achieve a low overpotential. Subsequently, the cathode morphology can affect the performance of Li-O_2 battery as well. As reported, during discharge, the generated Li_2O_2 cannot dissolve in organic electrolyte and deposits on the cathode, thus blocking the oxygen diffusion path, causing severe volume expansion of the electrode, leading to degradation of the electrode. As a solution, the porous structure of the cathode materials should be tuned. When coming to the topic about the activity, relevant content is discussed above and the detailed discussion is not mentioned for brevity.

Acknowledgements

This work was financially supported by National Program on Key Basic Research Project of China (2012CB215500 and 2014CB932300), Strategic Priority Research Program of the Chinese Academy of Sciences (Grant No. XDA09010404), National Natural Science Foundation of China (21422108, 21271168, and 51472232), Ministry of Science and Technology of the People's Republic of China (Grant No. 2016YFB0100100), and Jilin Province Science and Technology Development Program (grant nos. 20160101289JC).

Conflict of Interest

The authors declare no conflict of interest.

Keywords

design, electrocatalysts, electrochemical performance, Li-O_2 batteries

Received: March 30, 2017
Revised: May 11, 2017
Published online: September 18, 2017

[1] L. L. Zhang, X. S. Zhao, *Chem. Soc. Rev.* **2009**, *38*, 2520.
[2] C. P. Grey, J. M. Tarascon, *Nat. Mater.* **2016**, *16*, 45.
[3] S. Li, J. J. Niu, Y. C. Zhao, K. P. So, C. Wang, C. A. Wang, J. Li, *Nat. Commun.* **2014**, *6*, 7872.
[4] P. G. Bruce, S. A. Freunberger, L. J. Hardwick, J.-M. Tarascon, *Nat. Mater.* **2012**, *11*, 19.
[5] J.-J. Xu, Z.-L. Wang, D. Xu, L.-L. Zhang, X.-B. Zhang, *Nat. Commun.* **2013**, *4*, 2438.
[6] a) K. M. Abraham, Z. Jiang, *J. Electrochem. Soc.* **1996**, *143*, 1; b) L. Cecchetto, M. Salomon, B. Scrosati, F. Croce, *J. Power Sources* **2012**, *213*, 233; c) B. Horstmann, T. Danner, W. G. Bessler, *Energy Environ. Sci.* **2013**, *6*, 1299; d) H. Kitaura, H. Zhou, *Adv. Energy Mater.* **2012**, *2*, 889; e) M. Mehta, V. Bevara, P. Andrei, *J. Power Sources* **2015**, *286*, 299.
[7] Q.-C. Liu, J.-J. Xu, D. Xu, X.-B. Zhang, *Nat. Commun.* **2015**, *6*, 7892.
[8] R. S. Treptow, *J. Chem. Educ.* **2002**, *79*, 334.
[9] T. Ogasawara, A. Débart, M. Holzapfel, P. Novak, P. G. Bruce, *J. Am. Chem. Soc.* **2006**, *128*, 1390.
[10] a) H. Lim, E. Yilmaz, H. R. Byon, *J. Phys. Chem. Lett.* **2012**, *3*, 3210; b) H. Zheng, D. Xiao, X. Li, Y. Liu, Y. Wu, J. Wang, K. Jiang, C. Chen, L. Gu, X. Wei, Y.-S. Hu, Q. Chen, H. Li, *Nano Lett.* **2014**, *14*, 4245; c) J. T. Frith, A. E. Russell, N. Garcia-Araez, J. R. Owen, *Electrochem. Commun.* **2014**, *46*, 33.
[11] S. C. Ma, Y. Wu, J. W. Wang, Y. L. Zhang, Y. T. Zhang, X. X. Yan, Y. Wei, P. Liu, J. Wang, K. Jiang, S. S. Fan, Y. Xu, Z. Q. Peng, *Nano Lett.* **2015**, *15*, 8084.
[12] D. Y. Oh, J. F. Qi, B. H. Han, G. Zhang, T. J. Carney, J. Ohmura, Y. Zhang, Y. Shao-Horn, A. M. Belcher, *Nano Lett.* **2014**, *14*, 4837.

[13] W. Walke, V. Giordani, J. Uddin, V. S. Bryantsev, G. V. Chase, D. Addison, *J. Am. Chem. Soc.* **2013**, *135*, 2076.
[14] Y. Chen, S. A. Freunberger, Z. Peng, F. Barde, P. G. Bruce, *J. Am. Chem. Soc.* **2012**, *134*, 7952.
[15] Q.-C. Liu, J.-J. Xu, S. Yuan, Z.-W. Chang, D. Xu, Y.-B. Yin, L. Li, H.-X. Zhong, Y.-S. Jiang, J.-M. Yan, X.-B. Zhang, *Adv. Mater.* **2015**, *27*, 5241.
[16] J.-L. Shui, J. S. Okasinski, P. Kenesei, H. A. Dobbs, D. Zhao, J. D. Almer, D.-J. Liu, *Nat. Commun.* **2013**, *4*, 2255.
[17] B. D. McCloskey, D. Addison, *ACS Catal.* **2017**, *7*, 772.
[18] D. Aurbach, B. D. McCloskey, L. F. Nazar, P. G. Bruce, *Nat. Energy* **2016**, *1*, 1.
[19] Y. Li, X. Wang, S. Dong, X. Chen, G. L. Cui, *Adv. Energy Mater.* **2016**, *6*, 1600751.
[20] A. C. Luntz, B. D. McCloskey, *Chem. Rev.* **2014**, *114*, 11721.
[21] Z. Ma, X. X. Yuan, L. Li, Z.-F. Ma, D. P. Wilkinson, L. Zhang, J. J. Zhang, *Energy Environ. Sci.* **2015**, *8*, 2144.
[22] Z.-W. Chang, J.-J. Xu, Q.-C. Liu, L. Li, X.-B. Zhang, *Adv. Energy Mater.* **2015**, *5*, 1500633.
[23] F. Li, T. Zhang, H. Zhou, *Energy Environ. Sci.* **2013**, *6*, 1125.
[24] Y.-C. Lu, B. M. Gallant, D. G. Kwabi, J. R. Harding, R. R. Mitchell, M. S. Whittingham, Y. Shao-Horn, *Energy Environ. Sci.* **2013**, *6*, 750.
[25] a) Y. Chen, S. A. Freunberger, Z. Peng, F. Barde, P. G. Bruce, *J. Am. Chem. Soc.* **2012**, *134*, 7952; b) W. Walker, V. Giordani, J. Uddin, V. S. Bryantsev, G. V. Chase, D. Addison, *J. Am. Chem. Soc.* **2013**, *135*, 2076; c) B. D. Adams, R. Black, Z. Williams, R. Fernandes, M. Cuisinier, E. J. Berg, P. Novak, G. K. Murphy, L. F. Nazar, *Adv. Energy Mater.* **2014**, *5*, 1400867; d) S. A. Freunberger, Y. Chen, N. E. Drewett, L. J. Hardwick, F. Barde, P. G. Bruce, *Angew. Chem. Int. Ed.* **2011**, *50*, 8609.
[26] S. Flandrois, B. Simon, *Carbon* **1999**, *37*, 165.
[27] Y. Zhao, L. Y. P. Wang, M. T. Sougrati, Z. X. Feng, Y. Leconte, A. Fisher, M. Srinivasan, Z. C. Xu, *Adv. Energy Mater.* **2017**, 1601424.
[28] S. F. Wang, Y. J. Sha, Y. L. Zhu, X. M. Xu, Z. P. Shao, *J. Mater. Chem. A* **2015**, *3*, 16132.
[29] J. Kang, O. L. Li, N. H. Saito, *J. Power Sources* **2014**, *261*, 256.
[30] X. Yang, P. He, Y. Xia, *Electrochem. Commun.* **2009**, *11*, 1127.
[31] M. Mirzaeian, P. Hall, *Electrochim. Acta* **2009**, *54*, 7444.
[32] J. Q. Huang, B. Zhang, Y. Y. Xie, W. W. K. Lye, Z.-L. Xu, S. Abouali, M. A. Garakani, J.-Q. Huang, T.-Y. Zhang, B. L. Huang, J.-K. Kim, *Carbon* **2016**, *100*, 329.
[33] S. Liu, Z. Wang, C. Yu, Z. Zhao, X. Fan, Z. Linga, J. Qiu, *J. Mater. Chem. A* **2013**, *1*, 12033.
[34] J. H. Han, G. Huang, Y. Ito, X. W. Guo, T. S. Fujita, P. Liu, A. Hirata, M. W. Chen, *Adv. Energy Mater.* **2017**, 1601933.
[35] H. Kim, H. Lim, J. Kim, K. Kang, *J. Mater. Chem. A* **2014**, *2*, 33.
[36] Y. Li, J. Wang, X. Li, D. Geng, R. Li, X. Sun, *Chem. Commun.* **2011**, *47*, 9438.
[37] W. Zhou, H. Zhang, H. Nie, Y. Ma, Y. Zhang, H. Zhang, *ACS Appl. Mater. Interfaces* **2015**, *7*, 3389.
[38] H. Nie, H. Zhang, Y. Zhang, T. Liu, J. Li, Q. Lai, *Nanoscale* **2013**, *5*, 8484.
[39] X. Lin, L. Zhou, T. Huang, A. Yu, *J. Mater. Chem. A* **2013**, *1*, 1239.
[40] Z. Zhang, J. Bao, C. He, Y. Chen, J. Wei, Z. Zhou, *Adv. Funct. Mater.* **2014**, *24*, 6826.
[41] R. R. Mitchell, B. M. Gallant, C. V. Thompson, Y. ShaoHorn, *Energy Environ. Sci.* **2011**, *4*, 2952.
[42] J. Xiao, D. G. Mei, X. L. Li, W. Xu, D. Y. Wang, G. L. Graff, W. D. Bennett, Z. M. Nie, L. V. Saraf, I. A. Aksay, L. Lui, J.-G. Zhang, *Nano Lett.* **2011**, *11*, 5071.
[43] Z.-L. Wang, D. X, J-J. Xu, L.-L. Zhang, X.-B. Zhang, *Adv. Funct. Mater.* **2012**, *22*, 3699.
[44] H.-D. Lim, K.-Y. Park, H. Song, E. Y. Jang, H. Gwon, J. Kim, Y. H. Kim, M. D. Lima, R. O. Robles, X. Lepró, R. H. Baunhman, K. Kang, *Adv. Mater.* **2013**, *25*, 1348.
[45] Z. Y. Guo, D. D. Zhou, X. L. Dong, Z. J. Qiu, Y. G. Wang, Y. Y. Xia, *Adv. Mater.* **2013**, *25*, 5668.
[46] B. Sun, S. Q. Chen, H. Liu, G. Wang, *Adv. Funct. Mater.* **2015**, *25*, 4436.
[47] J. P. Paraknowitsch, A. Thomas, *Energy Environ. Sci.* **2013**, *6*, 2839.
[48] Y. L. Li, J. J. Wang, X. F. Li, D. S. Geng, M. N. Banis, Y. J. Tang, D. N. Wang, R. Y. Li, T.-K. Sham, X. L. Sun, *J. Mater. Chem.* **2012**, *22*, 20170.
[49] J.-H. Kim, A. G. Kannan, H.-S. Woo, D.-G. Jin, W. Kim, K. G. Ryu, D.-W. Kim, *J. Mater. Chem. A* **2015**, *3*, 18456.
[50] C. Y. Xu, J. C. Dai, X. G. Teng, Y. M. Zhu, *ChemCatChem* **2016**, *8*, 372.
[51] K. P. Gong, F. Du, Z. H. Xia, M. Durstock, L. M. Dai, *Science* **2009**, *323*, 760.
[52] C. Z. Shu, B. Li, B. S. Zhang, D. S. Su, *ChemSusChem* **2015**, *8*, 3973.
[53] G. Wu, N. H. Mack, W. Gao, S. Ma, R. Zhong, J. Han, J. K. Baldwin, P. Zelenay, *ACS Nano* **2012**, *6*, 9764.
[54] C. Z. Shu, Y. M. Lin, D. S. Su, *J. Mater. Chem. A* **2016**, *4*, 2128.
[55] J. H. Han, X. W. Guo, Y. K. Ito, P. Liu, D. Hojo, T. Aida, A. Hirata, T. Fujita, T. F. Adschiri, H. S. Zhou, M. W. Chen, *Adv. Energy Mater.* **2016**, *6*, 1501870.
[56] Z. Zhang, J. Bao, C. He, Y. N. Chen, J. P. Wei, Z. Zhou, *Adv. Funct. Mater.* **2014**, *24*, 6826.
[57] J. L. Shui, F. Du, C. M. Xie, Q. Li, L. M. Dai, *ACS Nano* **2014**, *8*, 2014.
[58] J. L. Shui, Y. Lin, J. W. Connell, J. T. Xu, X. L. Fan, L. M. Dai, *ACS Energy Lett.* **2016**, *1*, 260.
[59] C. T. Zhao, C. Yu, S. H. Liu, J. Yang, X. M. Fan, H. W. Huang, J. H. Qiu, *Adv. Funct. Mater.* **2015**, *25*, 6913.
[60] X. Ren, J. Zhu, F. Du, J. Liu, W. Zhang, *J. Phys. Chem. C* **2014**, *118*, 22412.
[61] X. Ren, B. Wang, J. Zhu, J. Liu, W. Zhang, Z. Wen, *Phys. Chem. Chem. Phys.* **2015**, *17*, 14605.
[62] F. Wu, Y. Xing, L. Li, J. Qian, W. J. Qu, J. G. Wen, D. Miller, Y. S. Ye, R. J. Chen, K. Amine, J. Lu, *ACS Appl. Mater. Interfaces* **2016**, *8*, 23635.
[63] Y.-C. Lu, Z. C. Xu, H. A. Gasteiger, S. Chen, K. Hamad-Schifferli, Y. Shao-Horn, *J. Am. Chem. Soc.* **2010**, *132*, 12170.
[64] H.-D. Lim, H. L. Song, H. K. Gwon, K.-Y. Park, J. S. Kim, Y. J. Bae, H. S. Kim, S.-K. Jung, T. W. Kim, Y. H. Kim, X. Lepro, R. Q. O-Robles, R. H. Baughman, K. Kang, *Energy Environ. Sci.* **2013**, *6*, 3570.
[65] J. Liu, R. Younesi, T. Gustafsson, K. Edström, J. F. Zhu, *Nano Energy* **2014**, *10*, 19.
[66] F. Wu, Y. Xing, X. Q. Zeng, Y. F. Yuan, X. Y. Zhang, R. S.-Yassar, J. G. Wen, D. J. Miller, L. Li, R. J. Chen, J. Lu, K. Amine, *Adv. Funct. Mater.* **2016**, *26*, 7626.
[67] V. R. Chitturi, M. Ara, W. Fawaz, K. Y. S. Ng, L. M. R. Arava, *ACS Catal.* **2016**, *6*, 7088.
[68] J. Lu, Y. Lei, K. C. Lau, X. Luo, P. Du, J. Wen, R. S. Assary, U. Das, D. J. Miller, J. W. Elam, H. M. Albishri, D. A. ElHady, Y.-K. Sun, L. A. Curtiss, K. Amine, *Nat. Commun.* **2013**, *4*, 2383.
[69] S. C. Ma, Y. Wu, J. W. Wang, Y. L. Zhang, Y. T. Zhang, X. X. Yan, Y. Wei, P. Liu, J. P. Wang, K. L. Jiang, S. S. Fan, Y. Xu, Z. Q. Peng, *Nano Lett.* **2015**, *15*, 8084.
[70] S. J. Ye, D. Y. Kim, D. W. Kim, O. O. Park, Y. K. Kang, *J. Mater. Chem. A* **2016**, *4*, 578.
[71] J. Wang, L. L. Liu, S. L. Chou, H. K. Liu, J. Z. Wang, *J. Mater. Chem. A* **2017**, *5*, 1462.
[72] F. Wu, Y. Xing, X. Q. Zeng, Y. F. Yuan, X. Y. Zhang, R. S-Yassar, J. G. Wen, D. J. Miller, L. Li, R. J. Chen, J. Lu, K. Amine, *Adv. Funct. Mater.* **2016**, *26*, 7626.
[73] X. Y. Lu, Y. Yin, L. Zhang, L. X. Xi, S. Oswald, J. W. Deng, *Nano Energy* **2016**, *30*, 69.

[74] X. Y. Lu, W. Q. Si, X. L. Sun, B. Liu, L. Zhang, C. L. Yan, O. G. Schmidt, *Nano Energy* **2016**, *19*, 428.
[75] B. Sun, P. Munroe, G. Wang, *Sci. Rep.* **2013**, *3*, 2247.
[76] B. Sun, X. Huang, S. Chen, P. Munroe, G. Wang, *Nano Lett.* **2014**, *14*, 3145.
[77] S. F. Tong, M. B. Zheng, Y. Lu, Z. X. Lin, X. P. Zhang, P. He, H. S. Zhou, *Chem. Commun.* **2015**, *51*, 7302.
[78] X. D. Lin, T. Cao, S. R. Cai, J. M. Fan, Y. J. Li, Q.-H. Wu, M. S. Zheng, Q. F. Dong, *J. Mater. Chem. A* **2016**, *4*, 7788.
[79] D. W. Su, D. H. Seo, Y. H. Ju, Z. J. Han, K. Ostrikov, S. Dou, H.-J. Ahn, Z. Q. Peng, G. X. Wang, *NPG Asia Materials* **2016**, *8*, e286.
[80] X. Guo, B. Sun, J. Q. Zhang, H. Liu, G. X. Wang, *J. Mater. Chem. A* **2016**, *4*, 9774.
[81] W. Zhou, Y. Cheng, X. F. Yang, B. S. Wu, H. J. Nie, H. Z. Zhang, H. M. Zhang, *J. Mater. Chem. A* **2015**, *3*, 14556.
[82] J. Lu, Y. J. Lee, X. Y. Luo, K. C. Lau, M. Asadi, H.-H. Wang, S. Brombosz, J. G. Wen, D. Y. Zhai, Z. H. Chen, D. J. Miller, Y. S. Jeong, J.-B. Park, Z. G. Z. Fang, B. D. Kumar, A. S.-Khojin, Y.-K. Sun, L. A. Curtiss, K. Amine, *Nature* **2016**, *529*, 377.
[83] X. Huang, H. Yu, H. Tan, J. X. Zhu, W. Y. Zhang, C. Y. Wang, J. Zhang, Y. X. Wang, Y. B. Lv, Z. Zeng, D. Y. Liu, J. Ding, Q. C. Zhang, M. Srinivasan, P. M. Ajayan, H. H. Hng, Q. Yan, *Adv. Funct. Mater.* **2014**, *24*, 6516.
[84] F. F. Tu, J. P. Hu, J. Xie, G. S. Cao, S. C. Zhang, S. Y. A. Yang, X. B. Zhao, H. Y. Yang, *Adv. Funct. Mater.* **2016**, *26*, 7725.
[85] G. Q. Wang, F. F. Tu, J. Xie, G. H. Du, S. C. Zhang, G. S. Cao, X. B. Zhao, *Adv. Sci.* **2016**, *3*, 1500339.
[86] H.-G. Jung, Y. S. Jeong, J.-B. Park, Y.-K. Sun, B. Scrosati, Y. J. Lee, *ACS Nano* **2013**, *7*, 3532.
[87] E. Yilmaz, C. Yogi, K. Yamanaka, T. Ohta, H. R. Byon, *Nano Lett.* **2013**, *13*, 4679.
[88] P. K. Bhattacharya, E. N. Nasybulin, M. H. Engelhard, L. Kovarik, M. E. Bowden, X. H. S. Li, D. J. Gaspar, W. Xu, J.-G. Zhang, *Adv. Funct. Mater.* **2014**, *24*, 7510.
[89] X. W. Guo, P. Liu, J. H. Han, Y. Ito, A. Hirata, T. S. Fujita, M. W. Chen, *Adv. Mater.* **2015**, *27*, 6137.
[90] Z. Y. Guo, D. D. Zhou, H. J. Liu, X. L. Dong, S. Y. Yuan, A. S. Yu, Y. G. Wang, Y. Y. Y. Xia, *J. Power Sources* **2015**, *276*, 181.
[91] C. Y. Jung, T. S. Zhao, L. Zeng, P. Tan, *J. Power Sources* **2016**, *331*, 82.
[92] K. R. Yoon, G. Y. Lee, J.-W. Jung, N.-H. Kim, S. O. Kim, I.-D. Kim, *Nano Lett.* **2016**, *16*, 2076.
[93] Y. Yang, W. Liu, Y. M. Wang, X. C. Wang, L. Xiao, J. T. Lu, L. Zhuang, *Phys. Chem. Chem. Phys.* **2014**, *16*, 20618.
[94] W.-B. Luo, X.-W. Gao, S.-L. Chou, J.-Z. Wang, H.-K. Liu, *Adv. Mater.* **2015**, *27*, 6862.
[95] Y.-J. Kang, S. C. Jung, H.-J. Kim, Y.-K. Han, S. H. Oh, *Nano Energy* **2016**, *27*, 1.
[96] L. M. Leng, J. Li, X. Y. Zeng, H. Y. Song, T. Shu, H. S. Wang, S. J. Liao, *J. Power Sources* **2017**, *337*, 173.
[97] W.-B. Luo, T. V. Pham, H.-P. Guo, H.-K. Liu, S.-X. Dou, *ACS Nano* **2017**, *11*, 1747.
[98] R. Black, J.-H. Lee, B. Adams, C. A. Mims, L. F. Nazar, *Angew. Chem. Int. Ed.* **2013**, *52*, 392.
[99] S. F. Wang, Y. J. Sha, Y. L. Zhu, X. M. Xu, Z. P. Shao, *J. Mater. Chem. A* **2015**, *3*, 16132.
[100] M. He, P. Zhang, S. Xu, X. B. Yan, *ACS Appl. Mater. Interfaces* **2016**, *8*, 23713.
[101] Y.-G. Huang, J. Chen, X.-H. Zhang, Y.-H. Zan, X.-M. Wu, Z.-Q. He, H.-Q. Wang, Q.-Y. Li, *Chem. Eng. J.* **2016**, *296*, 28.
[102] L. L. Zhang, F. F. Zhang, G. Huang, J. W. Wang, X. C. Du, Y. L. Qin, L. M. Wang, *J. Power Sources* **2014**, *261*, 311.
[103] S. Y. Liu, Y. G. Zhu, J. Xie, Y. Huo, H. Y. Yang, T. J. Zhu, G. S. Cao, X. B. Zhao, S. C. Zhang, *Adv. Energy Mater.* **2014**, *4*, 1301960.
[104] M. Hong, H. C. Choi, H. R. Byon, *Chem. Mater.* **2015**, *27*, 2234.
[105] S. F. Tong, M. B. Zheng, Y. Lu, Z. Lin, J. Li, X. P. Zhang, Y. Shi, P. He, H. S. Zhou, *J. Mater. Chem. A* **2015**, *3*, 16177.
[106] W.-J. Kwak, K. C. Lau, C.-D. Shin, K. Amine, L. A. Curtiss, Y.-K. Sun, *ACS Nano* **2015**, *9*, 4129.
[107] M. Asadi, B. D. Kumar, C. Liu, P. Phillips, P. Yasaei, A. Behranginia, P. Zapol, R. F. Klie, L. A. Curtiss, A. Salehi-Khojin, *ACS Nano* **2016**, *10*, 2167.
[108] M. W. Yin, S. T. Wu, X. D. Yang, W. Xia, Y. Shen, Y. H. Huang, A. Y. Cao, Q. Yuan, *ACS Nano* **2016**, *10*, 1240.
[109] Y. Lu, H. X. Ang, Q. Y. Yan, E. Fong, *Chem. Mater.* **2016**, *28*, 5743.
[110] C. Li, Z. Y. Guo, Y. Pang, Y. H. Sun, X. L. Su, Y. G. Wang, Y. Y. Xia, *ACS Appl. Mater. Interfaces* **2016**, *8*, 31638.
[111] H. T. Wu, W. Sun, Y. Wang, F. Wang, J. F. Liu, X. Y. Yue, Z. H. Wang, J. S. Qiao, D. W. Rooney, K. Sun, *ACS Appl. Mater. Interfaces* **2017**, *9*, 12355.
[112] S. C. Ma, L. Q. Sun, L. Cong, X. G. Gao, G. Yao, X. Guo, L. H. Tai, P. Mei, Y. P. Zeng, H. M. Xie, R. S. Wang, *J. Phys. Chem. C* **2013**, *117*, 25890.
[113] P.-X. Wang, L. Shao, N.-Q. Zhang, K.-N. Sun, *J. Power Sources* **2016**, *325*, 506.
[114] P. F. Li, W. Sun, Q. L. Yu, M. J. Guan, J. S. Qiao, Z. H. Wang, D. Rooney, K. Sun, *Mater. Lett.* **2015**, *158*, 84.
[115] J. F. Li, S. L. Xiong, Y. R. Liu, Z. C. Ju, Y. Qian, *ACS Appl. Mater. Interfaces* **2013**, *5*, 981.
[116] G. Q. Zhang, H. B. Wu, H. E. Hoster, M. B. Chan-Park, X. W. Lou, *Energy Environ. Sci.* **2012**, *5*, 9453.
[117] B. Sun, J. Q. Zhang, P. Munroe, H.-J. Ahn, G. X. Wang, *Electrochem. Commun.* **2013**, *31*, 88.
[118] B. Sun, X. D. Huang, S. Q. Chen, Y. F. Zhao, J. Q. Zhang, P. Munroe, G. X. Wang, *J. Mater. Chem. A* **2014**, *2*, 12053.
[119] B. Liu, P. F. Yan, W. Xu, J. M. Zheng, Y. He, L. L. Luo, M. E. Bowden, C.-M. Wang, J.-G. Zhang, *Nano Lett.* **2016**, *16*, 4932.
[120] H. Gong, H. R. Xue, T. Wang, H. Guo, X. L. Fan, L. Song, W. Xia, J. P. He, *ACS Appl. Mater. Interfaces* **2016**, *8*, 18060.
[121] Y. Luo, F. L. Lu, C. Jin, Y. Wang, R. Z. Yang, C. H. Yang, *J. Power Sources* **2016**, *319*, 19.
[122] L. L. Liu, J. Wang, Y. Y. Hou, J. Chen, H.-K. Liu, J. Z. Wang, Y. P. Wu, *Small* **2016**, *12*, 602.
[123] H. Gong, H. R. Xue, T. Wang, H. Guo, X. L. Fan, L. Song, W. Xia, J. P. He, *ACS Appl. Mater. Interfaces* **2016**, *8*, 18060.
[124] F. L. Qiu, P. He, J. Jiang, X. P. Zhang, S. F. Tong, H. S. Zhou, *Chem. Commun.* **2016**, *52*, 2713.
[125] W.-J. Kwak, T.-G. Kang, Y.-K. Sun, Y. J. Lee, *J. Mater. Chem. A* **2016**, *4*, 7020.
[126] D. Zhang, Y. Song, Z. Du, L. Wang, Y. Li, J. B. Goodenough, *J. Mater. Chem. A* **2015**, *3*, 9421.
[127] W. Yang, J. Salim, S. Li, C. Sun, L. Chen, J. B. Goodenough, Y. Kim, *J. Mater. Chem.* **2012**, *22*, 18902.
[128] Z. Ma, X. Yuan, L. Li, Z. F. Ma, *Chem. Commun.* **2014**, *50*, 14855.
[129] Z. Du, P. Yang, L. Wang, Y. Lu, J. B. Goodenough, J. Zhang, D. Zhang, *J. Power Sources* **2014**, *265*, 91.
[130] Z. Fu, X. Lin, T. Huang, A. Yu, *J. Solid State Electrochem.* **2012**, *16*, 1447.
[131] J. F. Cheng, M. Zhang, Y. X. Jiang, L. Zou, Y. P. Gong, B. Chi, J. Pu, L. Jian, *Electrochim. Acta* **2016**, *191*, 106.
[132] J.-J. Xu, Z.-L. Wang, D. Xu, F.-Z. Meng, X.-B. Zhang, *Energy Environ. Sci.* **2014**, *7*, 2213.
[133] J.-J. Xu, D. Xu, Z.-L. Wang, H.-G. Wang, L.-L. Zhang, X.-B. Zhang, *Angew. Chem. Int. Ed.* **2013**, *52*, 3887.
[134] G. Liu, H. B. Chen, L. Xia, S. Q. Wang, L.-X. Ding, D. D. Li, K. Xiao, S. Dai, H. H. Wang, *ACS Appl. Mater. Interfaces* **2015**, *7*, 22478.
[135] H. W. Park, D. U. Lee, M. G. Park, R. Ahmed, M. H. Seo, L. F. Nazar, *ChemSusChem* **2015**, *8*, 1058.

[136] F. Cheng, T. Zhang, Y. Zhang, J. Du, X. Han, J. Chen, *Angew. Chem., Int. Ed.* **2013**, *52*, 2474.
[137] J. I. Jung, H. Y. Jeong, M. G. Kim, G. Nam, J. Park, J. Cho, *Adv. Mater.* **2015**, *27*, 266.
[138] J. F. Cheng, M. Zhang, Y. X. Jiang, L. Zou, Y. P. Gong, B. Chi, J. Pu, L. Jian, *Electrochim. Acta* **2016**, *191*, 106.
[139] T. V. Pham, H. P. Guo, W. B. Luo, S. L. Chou, J. Z. Wang, H. K. Liu, *J. Mater. Chem. A.* **2017**, *5*, 5283.
[140] Z. D. Wang, Y. You, J. Yuan, Y.-X. Yin, Y.-T. Li, S. Xin, D. Zhang, *ACS Appl. Mater. Interfaces* **2016**, *8*, 6520.
[141] D. J. Chen, C. Chen, Z. M. Baiyee, Z. P. Shao, F. Ciucci, *Chem. Rev.* **2015**, *115*, 9869,.
[142] B. Hua, Y.-Q. Zhang, N. Yan, M. Li, Y.-F. Sun, J. Chen, J. Li, J.-L. Luo, *Adv. Funct. Mater.* **2016**, *26*, 4106.
[143] A. Grimaud, K. J. May, C. E. Carlton, Y.-L. Lee, M. Risch, W. T. Hong, J. Zhou, Y. Shao-Horn, *Nat. Commun.* **2013**, *4*, 2439.
[144] K. Jung, J. Lee, W. B. Im, S. Yoon, K. Shin, J. Lee, *Chem. Commun.* **2012**, *48*, 9406.
[145] Z. Ma, X. Yuan, L. Li, Z. Ma, *Chem. Commun.* **2014**, *50*, 14855.
[146] Y. H. Chen, S. A. Freunberger, Z. Q. Peng, O. Fontaine, P. G. Bruce, *Nat. Chem.* **2013**, *5*, 489.
[147] a) H. D. Lim, H. Song, J. Kim, H. Gwon, Y. Bae, K. Y. Park, J. Hong, H. Kim, T. Kim, Y. H. Kim, *Angew. Chem.* **2014**, *126*, 4007; b) H. D. Lim, H. Song, J. Kim, H. Gwon, Y. Bae, K. Y. Park, J. Hong, H. Kim, T. Kim, Y. H. Kim, *Angew. Chem. Int. Ed.* **2014**, *53*, 3926.
[148] B. J. J. Bergner, A. Schürmann, K. Peppler, A. Gausuch, J. Janek, *J. Am. Chem. Soc.* **2014**, *136*, 15054.
[149] D. Sun, Y. Shen, W. Zhang, L. Yu, Z. Q. Yi, W. Yin, D. Wang, Y. H. Huang, J. Wang, D. Wang, J. B. Goodenough, *J. Am. Chem. Soc.* **2014**, *136*, 8941.
[150] Z. J. Liang, Y.-C. Lu, *J. Am. Chem. Soc.* **2016**, *138*, 7574.
[151] Y. G. Zhu, X. Z. Wang, C. K. Jia, J. Yang, Q. Wang, *ACS Catal.* **2016**, *6*, 6191.
[152] D. P. Kundu, R. Black, B. Adams, L. F. Nazar, *ACS Cent. Sci.* **2015**, *1*, 510.
[153] X. W. Gao, Y. H. Chen, L. Johnson, P. G. Bruce, *Nat. Mater.* **2016**, *15*, 882.
[154] W.-H. Ryu, F. S. Gittleson, M. Schwab, T. H. Goh, A. D. Taylor, *Nano Lett.* **2015**, *15*, 434.
[155] X. W. Guo, P. Liu, J. H. Han, Y. Ito, A. Hirata, T. S. Fujita, M. W. Chen, *Adv. Mater.* **2015**, *27*, 6137.
[156] J. Q. Huang, B. Zhang, Y. Y. Xie, W. W. K. Lye, Z.-L. Xu, S. Abouali, M. A. Garakani, J.-Q. Huang, T.-Y. Zhang, B. L. Huang, J.-K. Kim, *Carbon* **2016**, *100*, 329.
[157] Q.-C. Zhu, S.-M. Xu, M. M. Harris, C. Ma, Y.-S. Liu, X. Wei, H.-S. Xu, Y.-X. Zhou, Y.-C. Cao, K.-X. Wang, J.-S. Chen, *Adv. Funct. Mater.* **2016**, *26*, 8514.
[158] T. Liu, J.-J. Xu, Q.-C. Liu, Z.-W. Chang, Y.-B. Yin, X.-Y. Yang, X. B. Zhang, *Small* **2017**, *13*, 1602952.
[159] X. L. Zhang, R. Gao, Z. Y. Li, Z. B. Hu, H. Y. Liu, X. F. Liu, *Electrochim. Acta* **2016**, *201*, 134.
[160] X. H. Yao, Q. M. Cheng, J. Xie, Q. Dong, D. W. Wang, *ACS Appl. Mater. Interfaces* **2015**, *7*, 21948.
[161] S. H. Oh, R. Black, E. Pomerantseva, J.-H. Lee, L. F. Nazar, *Nat. Chem.* **2012**, *4*, 1004.
[162] J.-H. Lee, R. Black, G. Popov, E. Pomerantseva, F. Nan, G. A. Botton, L. F. Nazar, *Energy Environ. Sci.* **2012**, *5*, 9558.
[163] F. Cheng, T. Zhang, Y. Zhang, J. Du, X. Han, J. Chen, *Angew. Chem., Int. Ed.* **2013**, *52*, 2474.
[164] T. Y. Ma, Y. Zheng, S. Dai, M. Jaroniec, S. Z. Qiao, *J. Mater. Chem. A* **2014**, *2*, 8676.
[165] R. Gao, L. Liu, Z. B. Hu, P. Zhang, X. Z. Cao, B. Y. Wang, X. F. Liu, *J. Mater. Chem. A* **2015**, *3*, 17598.
[166] R. Gao, Z. Y. Li, X. L. Zhang, J. C. Zhang, Z. B. H, X. F. Liu, *ACS Catal.* **2016**, *6*, 400.
[167] F. Wang, H. J. Li, Q. X. Wu, J. Fang, C. L. Yin, Y. H. Xu, *Electrochim. Acta* **2016**, *202*, 1.
[168] Y.-C. Lu, H. A. Gasteiger, Y. Shao-Hor, *J. Am. Chem. Soc.* **2011**, *133*, 19048.
[169] Y. Xu, W. A. Shelton, *J. Chem. Phys.* **2010**, *133*, 024703.
[170] G. K. P. Dathar, W. A. Shelton, Y. Xu, *J. Phys. Chem. Lett.* **2012**, *3*, 891.
[171] J.-B. Park, X. Y. Luo, J. Lu, C. D. Shin, C. S. Yoon, K. Amine, Y.-K. Sun, *J. Phys. Chem. C* **2015**, *119*, 15036.
[172] J. Lu, L. Cheng, K. C. Lau, E. Tyo, X. Y. Luo, J. G. Wen, D. Miller, R. S. Assary, H.-H. Wang, P. Redfern, H. M. Wu, J.-B. Park, Y.-K. Sun, S. Vajda, K. Amine, L. A. Curtiss, *Nat. Commun.* **2014**, *5*, 4895.
[173] J. Z. Zhu, X. D. Ren, J. J. Liu, W. Q. Zhang, Z. Y. Wen, *ACS Catal.* **2015**, *5*, 73.
[174] R. Gao, J. Z. Zhu, X. L. Xiao, Z. B. Hu, J. J. Liu, X. F. Liu, *J. Phys. Chem. C* **2015**, *119*, 4516.
[175] B. D. Adams, R. Black, C. Radtke, Z. Williams, B. L. Mehdi, N. D. Browning, L. F. Nazar, *ACS Nano* **2014**, *8*, 12483.
[176] J. Z. Zhu, F. Wang, B. Z. Wang, Y. W. Wang, J. J. Liu, W. Q. Zhang, Z. Y. Wen, *J. Am. Chem. Soc.* **2015**, *137*, 13572.
[177] Y. Q. Zheng, K. Song, J. Jung, C. Z. Li, Y.-U. Heo, M.-S. Park, M. H. Cho, Y.-M. Kang, K. J. Cho, *Chem. Mater.* **2015**, *27*, 3243.
[178] G.-H. Lee, S. Lee, J.-C. Kim, D. W. Kim, Y. K. Kang, D.-W. Kim, *Adv. Energy Mater.* **2016**, 1601741.
[179] H.-D. Lim, B. J. Lee, Y. P. Zheng, J. Y. Hong, J. S. Kim, H. Gwon, Y. M. Ko, M. Lee, K. Cho, K. Kang, *Nat. Energy* **2016**, *1*, 16066.
[180] Y. X. Hu, T. R. Zhang, F. Y. Cheng, Q. Zhao, X. P. Han, J. Chen, *Angew. Chem. Int. Ed.* **2015**, *54*, 4338.
[181] Z. Y. Guo, D. D. Zhou, H. J. Liu, X. L. Dong, S. Y. Yuan, A. S. Yu, Y. G. Wang, Y. Y. Xia, *J. Power Sources* **2015**, *276*, 181.
[182] Q.-C. Liu, J.-J. Xu, D. Xu, X.-B. Zhang, *Nat. Commun.* **2015**, *6*, 7892.
[183] X.-F. Yang, A. Wang, B. Qiao, J. Li, J. Y. Liu, T. Zhang, *Acc. Chem. Res.* **2013**, *46*, 1740.
[184] Y.-B. Yin, J.-J. Xu, Q.-C. Liu, X.-B. Zhang, *Adv. Mater.* **2016**, *28*, 7494.
[185] S. Lu, X. X. Bi, R. Tao, Q. Z. Wang, Y. Yao, F. Wu, C. Z. Zhang, *ACS Appl. Mater. Interfaces* **2017**, *9*, 4382.
[186] W.-H. Ryu, F. S. Gittleson, J. M. Thomsen, J. Y. Li, M. J. Schwab, G. W. Brudvig, A. D. Taylor, *Nat. Commun.* **2016**, *7*, 12925.
[187] B. G. Kim, S. J. Kim, H. S. Lee, J. W. Choi, *Chem. Mater.* **2014**, *26*, 4757.
[188] T. Inui, Y. Ono, Y. Takagi, J.-B. Kim, *Appl. Catal., A* **2000**, *202*, 215.
[189] S. J. Techner, *Appl. Catal.* **1990**, *62*, 1.
[190] L. Johnson, C. Li, Z. Liu, Y. H. Chen, S. A. Freunberger, P. C. Ashok, B. B. Praveen, K. Dholakia, J.-M. Tarascon, P. G. Bruce, *Nat. Chem.* **2014**, *6*, 1091.
[191] L. Luo, B. Liu, S. D. Song, W. Xu, J.-G. Zhang, C. M. Wang, *Nat. Nanotechnol.* https://doi.org/10.1038/NNANO.2017.27.
[192] J.-L. Shui, N. K. Karan, M. Balasbramanian, S.-Y. Li, D.-J. Liu, *J. Am. Chem. Soc.* **2012**, *134*, 16654.
[193] D. H. Deng, L. Yu, X. Q. Chen, G. X. Wang, L. Jin, X. L. Pan, J. Deng, G. Q. Sun, X. H. Bao, *Angew. Chem. Int. Ed.* **2013**, *52*, 371.
[194] J.-L. Shui, J. S. Okasinski, P. Kenesei, H. A. Dobbs, D. Zhao, J. D. Almer, D.-J. Liu, *Nat. Commun.* **2013**, *4*, 2255.
[195] R. S. Assary, J. Lu, P. Du, X. Luo, X. Zhang, Y. Ren, L. A. Curtiss, K. Amine, *ChemSusChem* **2013**, *6*, 51.
[196] H. Lee, D. J. Lee, J.-N. Lee, J. Song, Y. Lee, M.-H. Ryou, J.-K. Park, Y. M. Lee, *Electrochim. Acta* **2014**, *123*, 419.

